



# Bismuth Oxyhalide-Based Materials (BiOX: X = Cl, Br, I) and Their Application in Photoelectrocatalytic Degradation of Organic Pollutants in Water: A Review

## OPEN ACCESS

G. Xavier Castillo-Cabrera<sup>1,2</sup>, Patricio J. Espinoza-Montero<sup>1\*</sup>, Paulina Alulema-Pullupaxi<sup>1</sup>, José Ramón Mora<sup>3</sup> and Milton H. Villacís-García<sup>2</sup>

### Edited by:

Md. Mominul Islam,  
University of Dhaka, Bangladesh

### Reviewed by:

Weilong Shi,  
Jiangsu University of Science and  
Technology, China  
Mani Govindasamy,  
National Taipei University of  
Technology, Taiwan  
Weiguang Ma,  
Dalian Maritime University, China  
Dafeng Yan,  
Huazhong University of Science and  
Technology, China  
Jun Jin,  
China University of Geosciences  
Wuhan, China

### \*Correspondence:

Patricio J. Espinoza-Montero  
pespinoza646@puce.edu.ec

### Specialty section:

This article was submitted to  
Electrochemistry,  
a section of the journal  
Frontiers in Chemistry

Received: 21 March 2022

Accepted: 21 June 2022

Published: 11 July 2022

### Citation:

Castillo-Cabrera GX,  
Espinoza-Montero PJ,  
Alulema-Pullupaxi P, Mora JR and  
Villacís-García MH (2022) Bismuth  
Oxyhalide-Based Materials (BiOX: X =  
Cl, Br, I) and Their Application in  
Photoelectrocatalytic Degradation of  
Organic Pollutants in Water: A Review.  
Front. Chem. 10:900622.  
doi: 10.3389/fchem.2022.900622

<sup>1</sup>Escuela de Ciencias Químicas, Pontificia Universidad Católica Del Ecuador, Quito, Ecuador, <sup>2</sup>Facultad de Ciencias Químicas, Universidad Central Del Ecuador, Quito, Ecuador, <sup>3</sup>Universidad San Francisco de Quito, Quito, Ecuador

An important target of photoelectrocatalysis (PEC) technology is the development of semiconductor-based photoelectrodes capable of absorbing solar energy (visible light) and promoting oxidation and reduction reactions. Bismuth oxyhalide-based materials BiOX (X = Cl, Br, and I) meet these requirements. Their crystalline structure, optical and electronic properties, and photocatalytic activity under visible light mean that these materials can be coupled to other semiconductors to develop novel heterostructures for photoelectrochemical degradation systems. This review provides a general overview of controlled BiOX powder synthesis methods, and discusses the optical and structural features of BiOX-based materials, focusing on heterojunction photoanodes. In addition, it summarizes the most recent applications in this field, particularly photoelectrochemical performance, experimental conditions and degradation efficiencies reported for some organic pollutants (e.g., pharmaceuticals, organic dyes, phenolic derivatives, etc.). Finally, as this review seeks to serve as a guide for the characteristics and various properties of these interesting semiconductors, it discusses future PEC-related challenges to explore.

**Keywords:** photoelectrocatalysis, bismuth oxyhalide, visible-light, organic pollutants, water treatment

## 1 INTRODUCTION

Water pollution is an environmental problem that has attracted worldwide attention in recent years. Contaminants of emerging concern (CECs)—such as the active compounds in pharmaceuticals (antibiotics, pain relievers, etc.), personal care product, endocrine disrupting compounds, agrochemicals (herbicides, insecticides, fungicides, etc.), dyes, detergents (surfactants), and disinfection byproducts—are persistent organic molecules that can be found in wastewater, treated water, and natural water sources in concentrations ranging from mg/L to µg/L (Quesada et al., 2019; Gao et al., 2021; Li et al., 2021; Martínez-Huitle et al., 2015; Sanganyado et al., 2017; Garcia-Segura et al., 2020; Vasseghian et al., 2021; Zhang et al., 2021). CECs are generally complex and chemically stable molecules, which makes the removal process or degradation by traditional methods very complicated (Arotiba, Orimolade and Koiki, 2020). Currently, the consumption of inadequately treated water represents a risk to human health, as globally, approximately 700 million people do not have access to drinking water (Urban, 2017).

An underexplored area of water contamination research involves the active pharmaceutical compounds that appear after being metabolized by the body. These compounds are discarded in the form of metabolites, which are persistent in bodies of water (Quesada et al., 2019). Also contributing to water pollution are synthetic organic dyes, which are discharged into natural effluents mainly from the textile and paper industries (Nguyen et al., 2020). Another source of serious water pollution comes from the agricultural industry's indiscriminate use of agrochemicals, particularly synthetic pesticides, which, after being applied to plantations are transported by rainwater runoff to the main water bodies (Vasseghian et al., 2021). These organic pollutants remain in the environment and affect human health, because of their poor biodegradability and high levels of reactivity in the body, which leads to abnormal physiological processes (endocrine disruptors), enhanced bacteria resistance to antibiotics, and the appearance of certain types of cancer, as well as imbalanced chemical reactions in the body (Bagheri et al., 2017; Quesada et al., 2019). Therefore, the development of efficient technologies to completely remove or degrade stable organic pollutants is important. Several recent studies have reported relatively high effectiveness rates for the removal of organic contaminants in aqueous media, evaluating various techniques such as nanofiltration (Garcia-Ivars et al., 2017), ozonation (J. Wang & Bai, 2017), adsorption (Nguyen et al., 2020), photocatalysis (Quesada et al., 2019), and electrocatalysis (Singh and Goldsmith, 2020), the latter two being of special interest in the present review.

The development of photocatalysts for environmental remediation has been widely investigated, with emphasis on materials designed to harness solar energy (Hassani et al., 2021). However, a major disadvantage of photocatalysts is their photocatalytic efficiency, which is directly related to their intrinsic stability. On the other hand, photoelectrocatalysis (PEC) is an alternative that can substantially improve the limitations of photocatalytic processes. PEC consists of shining light on a semiconductor film, placed on a conductive substrate (photoelectrode), with a sufficient energy to overcome the energy barrier of the semiconductor band-gap ( $h\nu \geq E_g$ ). This energy promotes the formation of charge carriers; electrons ( $e^-$ ) migrate from the valence band towards the conduction band ( $e_{CB}^-$ ), leaving empty energetic states of electrons called "holes" ( $h^+$ ) in the valence band ( $h_{VB}^+$ ). Simultaneously, a potential perturbation is applied to prevent the recombination of electron/hole pairs ( $e_{CB}^-/h_{VB}^+$ ), which increase the availability of  $h_{VB}^+$  that promotes the generation of hydroxyl radicals ( $\cdot\text{OH}$ ) by water oxidation. The  $\cdot\text{OH}$  is the second strongest oxidant that exists in nature, and is responsible for oxidizing persistent organic matter, even to its total mineralization, **Figure 7** (Mousset and Dionysiou, 2020; Alulema-Pullupaxi, et al., 2021a; Wang et al., 2021; Wei et al., 2021). The most widely studied semiconductor material in this field is  $\text{TiO}_2$  (Xu et al., 2019; Alulema-Pullupaxi et al., 2021b; Sigcha-Pallo et al., 2022). However, due to its approximate band-gap energy of 3.2 eV, its application in photoelectrochemical processes with sunlight is limited, as this energy value corresponds to the UV range of the electromagnetic spectrum, which results in limited peak power

conversion. Therefore, interest in the development of new visible light active semiconductor materials with potential photoelectrocatalytic applications has grown in recent years. Of these materials, bismuth oxyhalides (BiOXs) stand out as novel materials for photocatalytic and photoelectrocatalytic applications (Gao et al., 2021).

BiOXs are p-type semiconductors, meaning the energetic arrangement of their conduction and valence bands means favor reduction processes over oxidation. Pristine BiOXs ( $X = \text{Cl, Br, I}$ ) are layered materials with an open crystal structure, exhibiting properties such as easy modification and formation of heterogeneous structures with other materials, chemical stability and ability to absorb UV and visible light because their narrow band-gaps (Gao et al., 2021; Wei et al., 2021). Due to these properties, when BiOXs couple with other semiconductors, the generated synergistic effect modifies their band structure and leads to oxidation processes, which is of particular interest for pollutant degradation. In this context, BiOX-based materials exhibit attractive properties for PEC. However, despite numerous studies on the development of BiOX-based photocatalysts, only a few of these materials have been applied in the degradation of organic pollutants through PEC (Li et al., 2021).

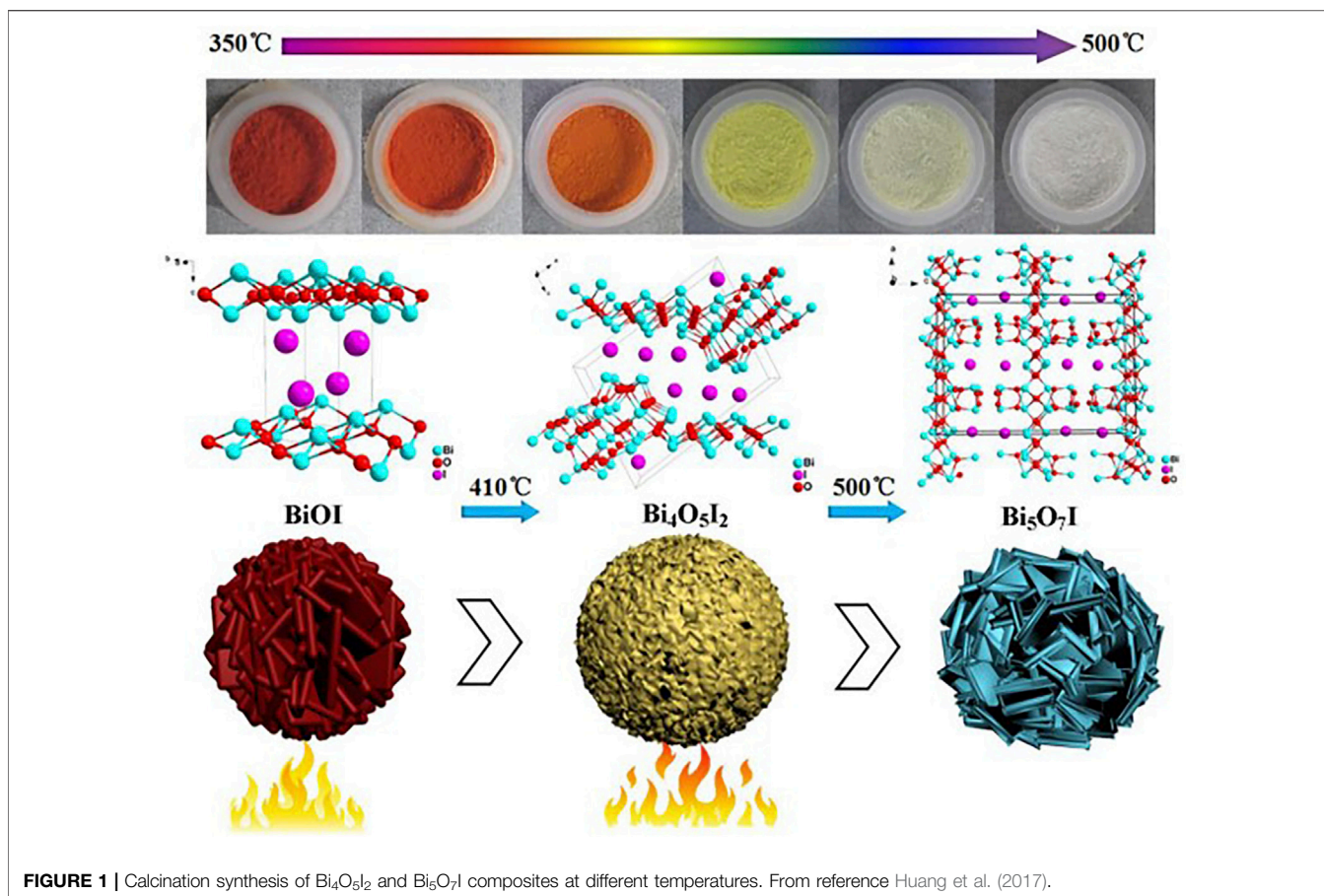
Based on the above, this review provides an overview of controlled BiOX powder synthesis methods, heterojunction formation and charge transfer mechanisms at the interface and the structural and optical properties of BiOX-based materials. Additionally, the most recent research on the photoelectrocatalytic degradation of organic pollutants is summarized, and future challenges in the development of semiconductor materials in PEC for environmental remediation are discussed.

## 2 BiOXs ( $X = \text{Cl, Br, I}$ ) SYNTHESIS METHODS

The controlled synthesis methods used to produce BiOXs depend on the desired structure and morphology. The following is an overview of reported BiOXs powder synthesis methods for different applications.

### 2.1 Hydrothermal/Solvothermal Method

The hydrothermal/solvothermal method is a soft chemical method using different solvents (hydrothermal: water; solvothermal: other solvents), in which pressure is generated to promote chemical reactions, increasing the reactivity and precursors solubility (Wei et al., 2021). The most common source of Bi using this method is bismuth nitrate pentahydrate ( $\text{Bi}(\text{NO}_3)_3 \cdot 5\text{H}_2\text{O}$ ), from which various micro and nanostructures with different BiOX compositions can be synthesized (Gao et al., 2021). For example, Xi Zhang et al. (2008) synthesized BiOXs powders ( $X = \text{Cl, Br, and I}$ ) by stirring a mixture containing  $\text{Bi}(\text{NO}_3)_3 \cdot 5\text{H}_2\text{O}$  dissolved in ethylene glycol and inorganic salts of the halogens (KCl, NaBr, and KI) for 30 min; after autoclave heating at 160°C under self-generated pressure, the precipitates were collected, washed, and dried at 50°C. Thus, by controlling



the kinetic and thermodynamic parameters of the reaction, the semiconductors' morphology, crystalline phase, size, and composition can be adjusted. This method is versatile, as various suitable solvent can be used for synthesis, the choice of solvent not only determines the morphological characteristics of  $\text{BiOXs}$ , but also allows control of the particle size during crystal growth.

## 2.2 Hydrolysis Method

Unlike the hydro/solvothermal method, in synthesis *via* hydrolysis, several bismuth salts can be used as precursors, including halides, nitrates, and oxides. However, controlling the reaction to obtain dimensionally uniform products is more complicated, even when the reaction conditions are not severe (Wei et al., 2021). The precursor compounds, greatly impact the morphology and yield in the synthesis of these catalysts. Additionally, the solvent affects crystal growth, which is an important factor in photocatalytic performance (Li et al., 2021). Using direct hydrolysis, Su et al. (2014) synthesized bismuth oxyiodide ( $\text{BiOI}$ ) with a hierarchical flower-like structure with  $\text{BiI}_3$  as a precursor. The hydrolysis method is suitable to prepare photoelectrodes using electrodeposition techniques, and the reaction medium also serves as an electrochemical medium for electrode modification. Electrodepositions with  $\text{BiOX}$  have been tested especially on

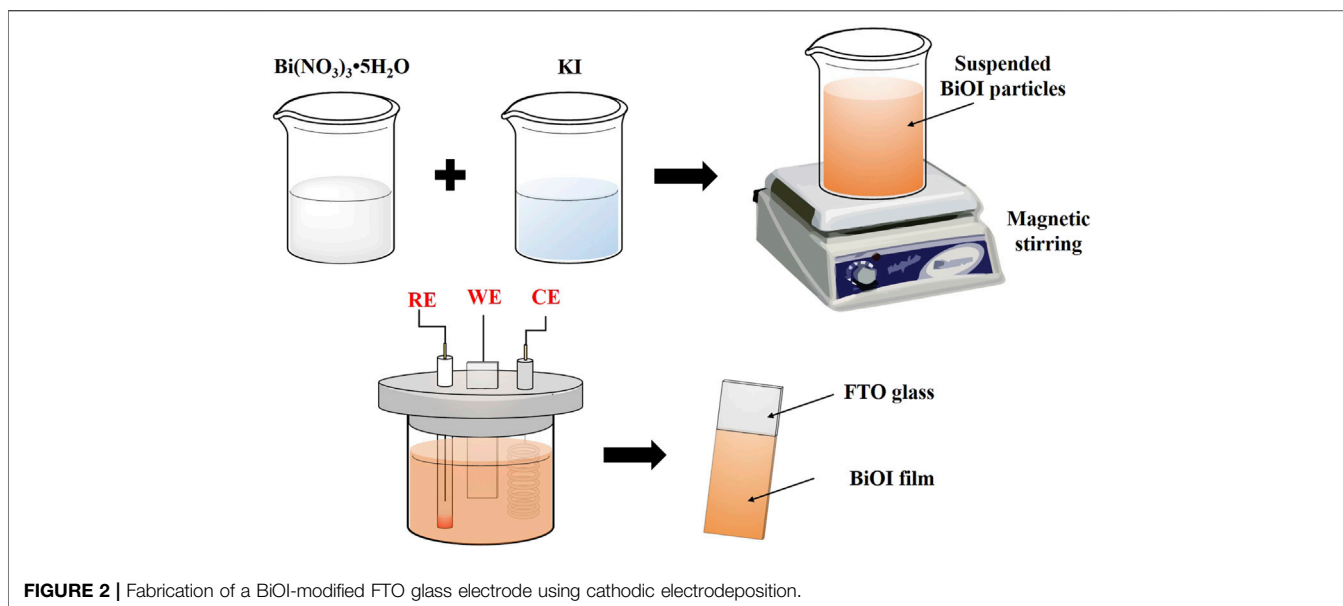
fluorine-doped tin oxide (FTO) and indium tin oxide (ITO) electrodes (Ling et al., 2020).

## 2.3 Calcination Method

Calcination is a useful method when a phase transformation of the bismuth oxyhalide to a bismuth-rich bismuth oxyhalide is desired, as heating removes unstable halogen atoms in the crystal structure (Gao et al., 2021; Wei et al., 2021). Using this method, Huang et al. (2017) synthesized  $\text{Bi}_4\text{O}_5\text{I}_2$ ,  $\text{Bi}_5\text{O}_7\text{I}$ , and  $\text{Bi}_4\text{O}_5\text{I}_2$ - $\text{Bi}_5\text{O}_7\text{I}$  composites using  $\text{BiOI}$  as the precursor (**Figure 1**). Calcination temperatures were set at 350, 380, 410, 440, 470, and 500°C. After heating, the samples were collected and characterized by *x*-ray diffraction (XRD); the diffraction patterns indicated the phase transformation of  $\text{BiOI}$ . In another study, Lee et al. (2015) described the synthesis of some bismuth-rich  $\text{BiOI}$ -based composites via hydrothermal methods without the need for calcination.

## 2.4 Ultrasound-Assisted Method

Ultrasound has been used to complement to traditional methods of producing  $\text{BiOX}$ -based composites, such as the spray-assisted method. Using a hydrothermal method, Qin et al. (2020) fabricated a  $\text{BiOI}/\text{Bi}_2\text{O}_4$  Z-type heterojunction by subjecting different amounts of  $\text{Bi}_2\text{O}_4$  (input power of 300 W and a frequency of 40 kHz) to ultrasound for 1 hour. Morphology

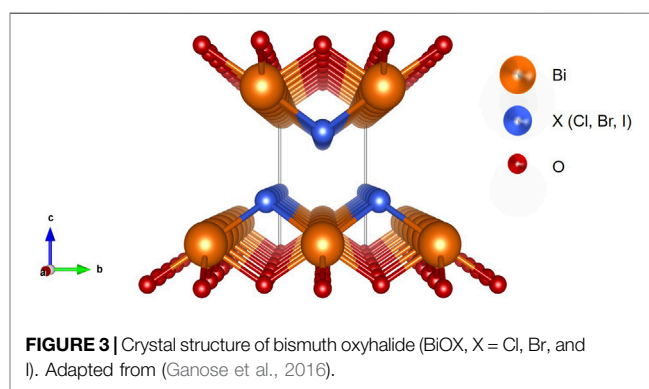


results of this material showed that the  $\text{Bi}_2\text{O}_4$  structure was irregular and consisted of nanorods of various sizes. Meanwhile, the structure of BiOI was hierarchical with agglomerations of flower-like nanosheets. This composite exhibited excellent visible light properties for the degradation of Rhodamine B (RhB) in a photocatalytic system.

In photoelectrocatalytic processes, the design of a stable and functional photoelectrode based on a suitable semiconductor is important. Potentiostatic cathodic electrodeposition is one of the most common techniques to create BiOX-modified electrodes. In a typical three-electrode system, the working electrode (commonly FTO or ITO), the reference electrode and the counter electrode are placed in a reaction medium, usually a hydrolysis synthesis medium. (Ye et al., 2015; Orimolade and Arotiba, 2022). A suitable potential difference is applied at a specific time (depending on the material), and the BiOX particles migrate to the electrode and deposit on its surface, covering it with a thin film. The coupling of BiOX with the electrode (another semiconductor) creates the so-called BiOX-based material, which has a potential role in electrochemical, photochemical, and photoelectrochemical processes. **Figure 2** presents a simple schematic of the electrodeposition of BiOI on a typical FTO electrode. Other methods to produce photoelectrodes have been successfully employed, such as the SILAR method (Ma et al., 2021), chemical bath deposition (Zhang et al., 2020), and the dipping process (Cong et al., 2017).

### 3 BiOX-BASED MATERIALS

BiOXs belong to the class of ternary semiconducting materials of group V-VI-VII; they crystallize in a tetragonal matlockite structure with a perfect (001) facet (Gao et al., 2021; Wei et al., 2021). As illustrated in **Figure 3**, these halogen-modified bismuth oxides are layered materials, that is, they consist of



$[\text{Bi}_2\text{O}_2]^{2+}$  layers successively intercalated with double layers of halide  $\text{X}^-$  ions linked by Van der Waals interactions (Ganose et al., 2016). This layered structure gives them an intrinsic stability, since a space is formed between layers, which polarizes the atoms and orbitals to obtain a dipole that can separate the photogenerated charges and prevent their recombination. This last feature is of great interest in both photocatalytic and photoelectrocatalytic processes (Zhao et al., 2012).

Among the most widely used semiconductor materials in PEC,  $\text{TiO}_2$  is the mostly known, due to its stability, friendliness, non-toxicity, and wide availability (Olea et al., 2021). However,  $\text{TiO}_2$  has a wide band-gap potential ( $\sim 3.2$  eV vs. NHE), which limits its applications in PEC. To compensate for this disadvantage, some photocatalysts have narrower band-gaps, which can absorb the visible light spectrum and limit the recombination of the photogenerated charge carriers (**Figure 4**). It is relevant to note that most of these semiconductor materials are generally used in the production of photoanodes (for oxidation reactions). These materials belong to the n-type semiconductors, where the conduction band is relatively full of electrons that are then

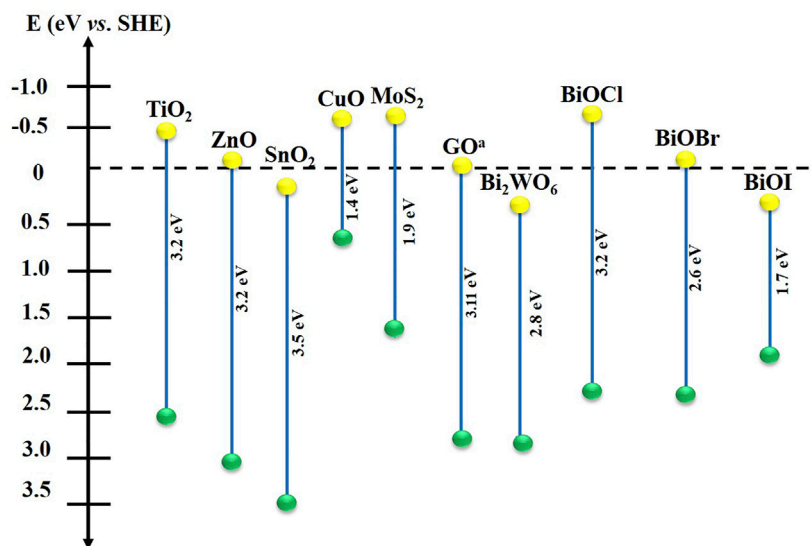


**FIGURE 4** | Band-gap of various semiconductor materials. Valence band (green); conduction band (yellow). <sup>a</sup> Graphene oxide. Adapted from: (Kumar et al., 2021; Olea, Bueno and Pérez, 2021).

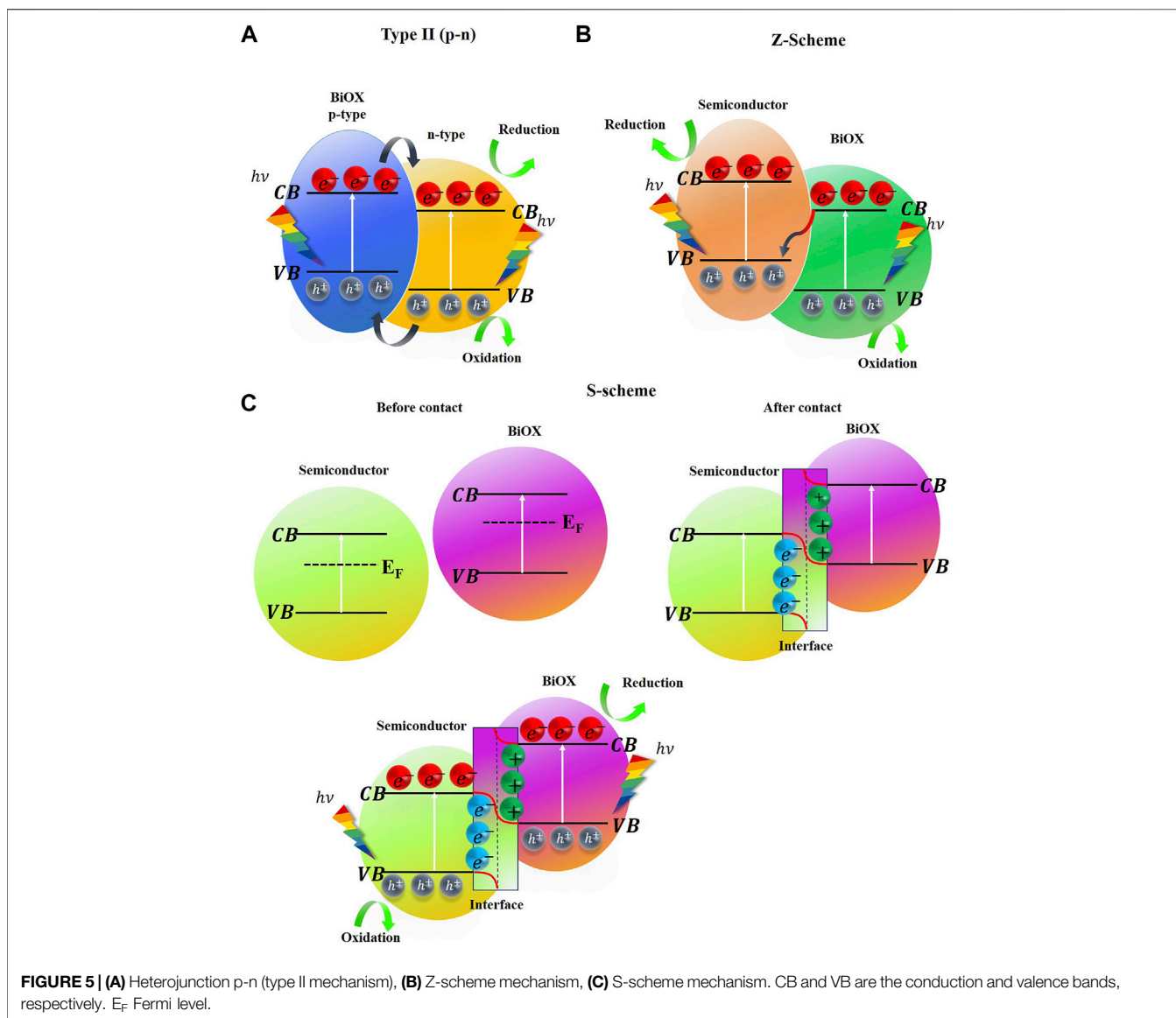
transported by an external circuit in photoelectrocatalytic processes. Additionally, the photogenerated holes must have a sufficient anodic potential to produce  $\bullet\text{OH}$  when they react with the aqueous medium (Olea et al, 2021). On the other hand, p-type semiconductors such as CuO and pristine BiOX (Ye et al., 2015), have valence band relatively full of positive vacancies ( $\text{h}^+$ ), these materials are used for reduction reactions (photocathode production) (Kusmierek, 2020; Olea et al., 2021). Thus BiOX-based photoanodes have been designed to improve the optical and performance properties of n-type semiconductors, including TiO<sub>2</sub> and various others (Figure 4).

To overcome the limitations of n-type semiconductors in photocatalytic and photoelectrocatalytic processes, the formation of heterojunctions with BiOXs has been considered an excellent option. The formation of heterostructures results in a strategy to carrier separation and decrease the recombination rate (Li et al., 2020). Heterojunctions result from the interaction between two semiconductors with different band-gaps. The Fermi levels of both semiconductors align at the interface, and the conduction and valence bands bend toward different energy levels (Kumar et al., 2021; Olea et al, 2021). Heterojunctions can be classified by the charge transfer mechanism at the interface or by the types of semiconductors that form the heterojunction. The p-n type heterojunction formed by the coupling of an n-type semiconductor and a p-type semiconductor is in agreement with the type II mechanism (Ye et al., 2015).

In this regard, Guo et al. (2020) fabricated a Bi<sub>2</sub>WO<sub>6</sub>/BiOCl heterostructure using a solvothermal method with excellent photochemical performance. The separation and charge transfer along the interface between the semiconductors showed that electrons flowed from Bi<sub>2</sub>WO<sub>6</sub> to BiOI according to the type II mechanism (Figure 5A), as modeled by electron difference density. In addition, the internal electric field of BiOCl further enhances charge separation. Similar results for the

Bi<sub>2</sub>WO<sub>6</sub>/BiOBr heterojunction synthesized using a two-step ionic liquid-assisted method showed that charge transfer occurred, evidenced by the irregular BiOBr structure adhering to the flower-like morphology of Bi<sub>2</sub>WO<sub>6</sub> (Pancielejko et al., 2021). Another heterostructure modification with BiOX has involved composites incorporated with carbonaceous materials. Due to their hierarchical structures and large active areas, the Bi-C bonds increase the speed of electron mobility between the bands (Hou et al., 2017). For example, Rashid et al. (2020) used a simple hydrothermal method to synthesize a BiOCl/GO composite (GO: graphene oxide). As shown in Figure 4, BiOCl is not active against visible light; however, by adding GO, the band-gap shifted towards 3.08 eV, which promote catalytic reactions in the medium even under sunlight irradiation. Although BiOX-based composites appear to improve charge transport at the heterojunction interface, the incorporation of defects in BiOXs' crystal structure has been examined, and results have shown promising applications in other fields of advanced oxidation processes (Shi et al., 2021).

Another type of BiOX-based heterojunction is the Z-scheme (Figure 5B), in which only electrons from the conduction band of the n-type semiconductor are directed toward the valence band of the p-type semiconductor (Y. Li et al., 2021). The type of heterojunction produced depends on the involved the photocatalysts' band structure, their electronic nature, and the potential levels at which the reactions occur. In this context, Qin et al. (2020) designed a BiOI/Bi<sub>2</sub>O<sub>4</sub> heterojunction using an ultrasound-assisted hydrothermal method. Because the valence band of BiOI was more positive than the reduction potential of  $\text{OH}^-/\bullet\text{OH}$  and the conduction band of Bi<sub>2</sub>O<sub>4</sub> was more negative than the oxidation potential of  $\text{O}_2/\text{O}_2^{\bullet-}$ , the possible mechanism for charge transport consisted of electrons from the conduction band of BiOI migrate to the valence band of Bi<sub>2</sub>O<sub>4</sub> to neutralize the photoexcited holes (Z-scheme). Another effective



heterojunction charge transfer mechanism is the S-scheme (**Figure 5C**). Herein, two semiconductors—one dedicated to oxidation reactions (more positive valence band) and one reduction semiconductor (more negative conduction band)—come together and generate an interface with a strong redox potential; this is because, the photoexcited electrons are kept in the conduction band of the reduction photocatalyst and the holes are kept in the valence band of the oxidizing photocatalyst (Xu et al., 2020). In addition, a spontaneous diffusion of the remaining electrons and holes from the reducing semiconductor to the oxidizing semiconductor and vice versa occurs, causing the bands to bend in the interface to maintain Fermi level equilibrium (Liao et al., 2021). Related studies have examined the S-scheme heterojunction of the ternary composite  $\text{Bi}_7\text{O}_9\text{I}_3/\text{g-C}_3\text{N}_4/\text{Bi}_3\text{O}_4\text{Cl}$  synthesized via the oil bath method (Yuan et al., 2022). This composite has a double interface between the oxyhalides and  $\text{g-C}_3\text{N}_4$ . Electrons migrate from  $\text{g-C}_3\text{N}_4$

towards  $\text{Bi}_7\text{O}_9\text{I}_3$  and  $\text{Bi}_3\text{O}_4\text{Cl}$  simultaneously, causing band bending up and down the interface. This result in charge transfer and recombination blocking solely at the interface, leaving only electrons and holes with strong redox capabilities for light promoted reactions (Yuan et al., 2022). In this and other cases  $\text{g-C}_3\text{N}_4$  acts as a kind of charge carrier at the conducting interface (Yan, Liu and Jin, 2021), strengthening the internal electric field and preventing recombination when light acts on the photocatalysts. This also includes quaternary BiOX-based composites, such as  $\text{BiO}_x\text{Cl}_y/\text{BiO}_m\text{Br}_n/\text{BiO}_p\text{I}_q/\text{g-C}_3\text{N}_4$  (Lin et al., 2022). Further, a heterostructure formed by coupling a noble metal with a semiconductor forms a typical Schottky junction (Bai et al., 2015), wherein the metal concentrates the photogenerated holes of the p-type semiconductor (BiOX). In this way, a so-called Schottky barrier is formed which prevents the return of charge carriers from the metal back to the semiconductor, that is, the charge flow occurs unidirectionally

(Bai et al., 2015; Kumar et al., 2021). In this context, Orimolade and Arotiba, (2022) fabricated a functional BiOI photoelectrode decorated with Ag nanoparticles supported on FTO glass. By loading silver particles on the BiOI/FTO electrode, the photocurrent responses increased. This is attributed to Ag acting as a photosensitizer by absorbing photons and controlling direct electron transfer.

### 3.1 Band Structure

Theoretical studies based on *ab initio* calculations can successfully predict some electronic, optical and structural properties of these materials (BiOX). Some of these properties are related to the formation of continuous bands of energy levels (atomic orbitals). One of the most important advantages of semiconductor materials over other photocatalysts is their narrow band-gap energy. Poznyak and Kulak, (1990) were the first to analyze the photoelectrochemical properties of BiOX using an anodic bismuth oxidation method; they synthesized BiOX films ( $X = \text{Cl, Br, and I}$ ), finding band-gap values of 3.50 eV (BiOCl), 2.92 eV (BiOBr) and 1.90 eV (BiOI). These band-gap energy values have been confirmed by computational calculations employing density functional theory (DFT) (Zhao et al., 2012). The valence band maximum of BiOX consists of  $np$  orbitals of the halogens ( $n = 3, 4, \text{ and } 5$  for Cl, Br, and I, respectively) and  $2p$  orbitals of oxygen, while the conduction band minimum contains  $6p$  orbitals of bismuth (Zhao et al., 2012). Recently, Barhoumi and Said (2021) theoretically examined the band structures of BiOXs, including BiOF, using the generalized gradient approximation (GGA) and GW approximation (GWA), supported by density functional theory (DFT), obtaining band-gap results more in line with those reported experimentally, from 2.33 eV for BiOI to 4.04 eV for BiOF.

### 3.2 Crystal Structure and Optical Properties

Although BiOXs exhibit narrow band-gap energies and good activity under visible light, their low quantum efficiency limits their applications in both photocatalysis and PEC because of the high recombination rate of photogenerated  $e_{\text{CB}}^-/h_{\text{VB}}^+$  pairs (Cao et al., 2018; Chen et al., 2018). To improve their optical properties and reduce charge recombination, doping, surface modification, and heterojunction formation have been adopted as alternatives to accelerate charge transfer and increase efficiency in PEC degradation applications (Li et al., 2021; Wang et al., 2021). In recent years, many studies have been reported discussing the optical and structural properties of BiOX-based materials from a DFT-based theoretical perspective, including indium-doped BiOX (Li et al., 2018),  $\text{MoS}_2/\text{BiOX}$  ( $X = \text{Cl, Br, and I}$ ) heterojunctions (Gao et al., 2019), BiOCl/BiOBr (Cui et al., 2019; Li et al., 2021), and stoichiometric low-index BiOI surfaces (Dai and Zhao, 2017).

#### 3.2.1 Crystalline Phase and Morphology

The stability of BiOXs is mainly due to their layered structure, a feature that promotes the formation of new structures with other semiconducting materials. Q. Wang et al. (2019) prepared a Bi-modified BiOI- $\text{Bi}_2\text{O}_3$  heterojunction using an *in situ* reduction

method applying UV light with BiOI- $\text{Bi}_2\text{O}_3$  previously prepared by single immersion at room temperature method reported by Cong et al. (2017). Using high-resolution transmission electron microscopy (HRTEM), the morphology of the Bi/BiOI- $\text{Bi}_2\text{O}_3$  film was investigated; results, showed that the  $\text{Bi}^0$  (012) planes and BiOI (110) planes were predominant, where  $\text{Bi}^0$  was in direct contact with BiOI. On the other hand, Xu et al. (2020) synthesized stoichiometric  $\text{BiOCl}_x\text{I}_{1-x}$  ( $x = 1.0, 0.75, 0.5, \text{ and } 0.25$ ) using an alcoholysis method at room temperature. XRD showed that the percentage exposure of the (001) crystalline plane (matlockite) was predominant in the  $\text{BiOCl}_x\text{I}_{1-x}$  solid solutions. Moreover, when the stoichiometric value  $x$  decreased, the crystalline parameters  $a$  and  $c$  of  $\text{BiOCl}_x\text{I}_{1-x}$  tended to increase, because the interlayer spacing of the crystal structure expanded as I atoms replaced Cl atoms. Using field emission scanning electron microscopy (FESEM), they found that the synthesized  $\text{BiOCl}_x\text{I}_{1-x}$  materials exhibited a two-dimensional flake-like structure, which when stacked irregularly formed microsphere or flower-like architectures. Furthermore, C. Zhao et al. (2021) successfully prepared a  $\text{Bi}_5\text{O}_7\text{I}/\text{UiO}-66\text{-NH}_2$  ( $\text{UiO}-66\text{-NH}_2$  is a zirconium organometallic) heterojunction through a ball milling method.  $\text{Bi}_5\text{O}_7\text{I}$  synthesized using a calcination method of BiOI prepared by co-precipitation was characterized by XRD;  $\text{Bi}_5\text{O}_7\text{I}$  exhibited high crystallinity. Scanning electron microscopy (SEM), transmission electron microscopy (TEM) and HRTEM results showed that  $\text{Bi}_5\text{O}_7\text{I}$  had a three-dimensional coral-like structure built by nanorods that formed agglomerations (Figure 6). Additionally, the microscopy results suggested that the closed interaction of the  $\text{Bi}_5\text{O}_7\text{I}/\text{UiO}-66\text{-NH}_2$  heterojunction promoted the transfer of photogenerated charges, thus increasing the rate of catalytic reactions. In another study, Pancielejko et al. (2021) prepared a  $\text{Bi}_2\text{WO}_6/\text{BiOBr}$  heterojunction based on a two-step synthesis. Ultraviolet-visible diffuse reflectance spectroscopy (UV-vis DRS) results showed that increasing the amount of BiOBr the response to visible light is decreased, because  $\text{Bi}_2\text{WO}_6$  surface was completely covered, causing light shielding. Thus, the synthesis method plays an important role in the structure, morphology, and stoichiometry of the desired BiOX. Many photocatalysts are limited by their supporting material, since physical interaction with their surface would modify their morphology. As BiOX are layered materials, a semiconducting surface with a large number of irregular interstices could affect the stability of the resulting material.

#### 3.2.2 Optical Properties

The ability of BiOXs to absorb light in the visible spectrum plays a key role in their photocatalytic activity (Wilczewska et al., 2021). The success of BiOX-based materials in photocatalytic and photoelectrocatalytic applications is related to the hierarchy of their surface structures, which significantly improve the ability to absorb visible light with respect to BiOXs. In this regard, using an *in situ* chemical deposition-precipitation method, Wang et al. (2020) synthesized a 2D/2D BiOBr/ $\text{Bi}_{12}\text{O}_{17}\text{Cl}_{12}$  heterojunction and evaluated its photocatalytic ability regarding the degradation of pollutants in water. Based on Tauc plots, they obtained a band-gap energy of 2.28 eV for the BiOBr/ $\text{Bi}_{12}\text{O}_{17}\text{Cl}_{12}$  composite. Additionally, they investigated the light absorption ability with

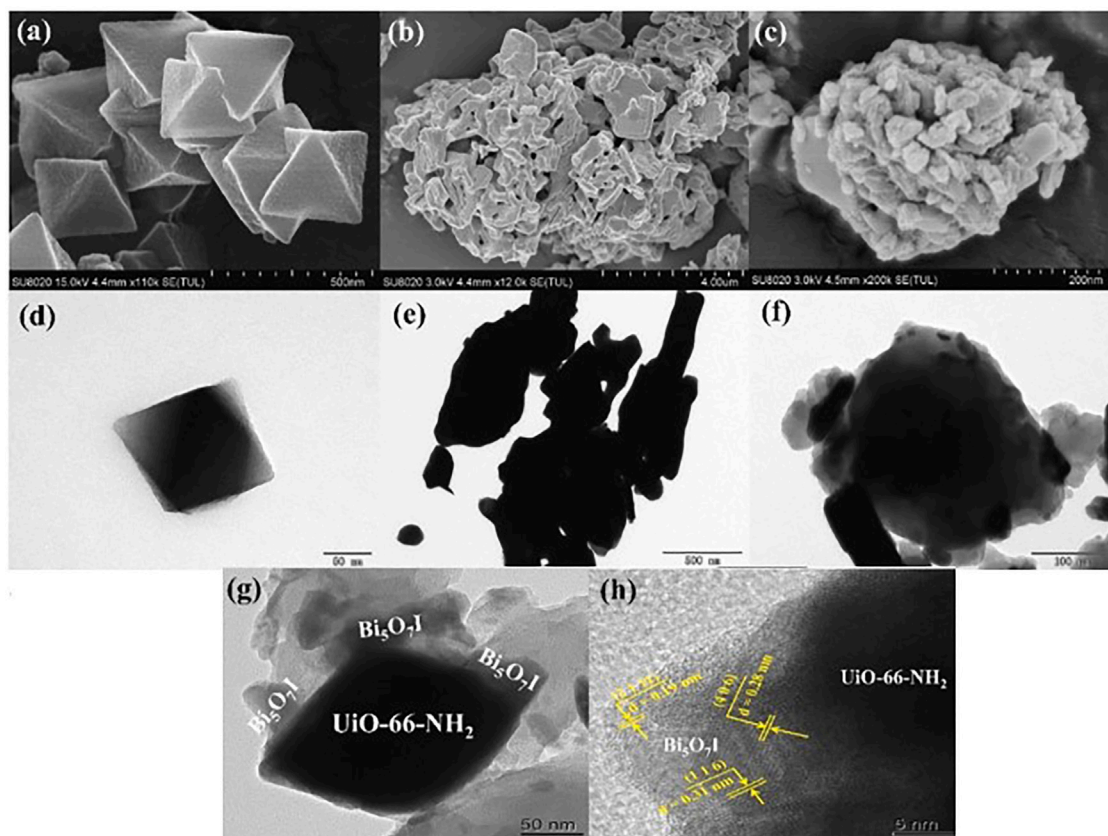


**FIGURE 6 | (A,D)** SEM and TEM micrographs of UiO-66-NH<sub>2</sub>, **(B,E)** Bi<sub>5</sub>O<sub>7</sub>I, **(C,F)** BU-5, and **(G,H)** HRTEM. From reference (Zhao et al., 2021).

UV-vis DRS and observed the two-dimensional structure of BiOBr/Bi<sub>12</sub>O<sub>17</sub>Cl<sub>12</sub> exhibited a significant enhancement in visible light absorption, as the absorption edge was red-shifted by approximately 530 nm, whereas pure BiOBr exhibited poor absorption (~430 nm of the absorption edge). Similar results previously reported by Lee et al. (2019) for a t-PbBiO<sub>2</sub>/Bi<sub>5</sub>O<sub>7</sub>I/g-C<sub>3</sub>N<sub>4</sub> composite prepared using hydrothermal processes, showed that introducing g-C<sub>3</sub>N<sub>4</sub> into the t-PbBiO<sub>2</sub>/Bi<sub>5</sub>O<sub>7</sub>I structure improved the visible light response and efficiently promoted photogenerated charge carriers. Likewise, Wu et al. (2019) developed BiOCl/Mo<sub>2</sub>S composites using ultrasound-assisted synthesis, the interfacial formation of Bi-S bonds, charge separation and significant reduction of band-gap energy were promoted due to the formation of oxygen vacancies. Oxygen vacancy refers to a type of defect in semiconductor oxides (Huang et al., 2014). The band-gap energy of the composites was located between 3.45 and 3.03 eV and decreased as MoS<sub>2</sub> mass ratio increased. Furthermore, using an *in situ* synthesis method, Qi et al. (2021) prepared a heterogeneous WS<sub>2</sub>/Mo<sub>2</sub>S/BiOCl structure and showed that by increasing the stoichiometric ratio of WS<sub>2</sub>/Mo<sub>2</sub>S, the light absorption band edge increased while BiOCl's activity against light was enhanced. In a similar study, Liu et al. (2021) synthesized S-doped BiOBr (S-BiOBr) using a solvothermal method; DRS showed that the 0.5S-BiOBr (0.5S refers to sulfur mass ratio) doping exhibited high visible

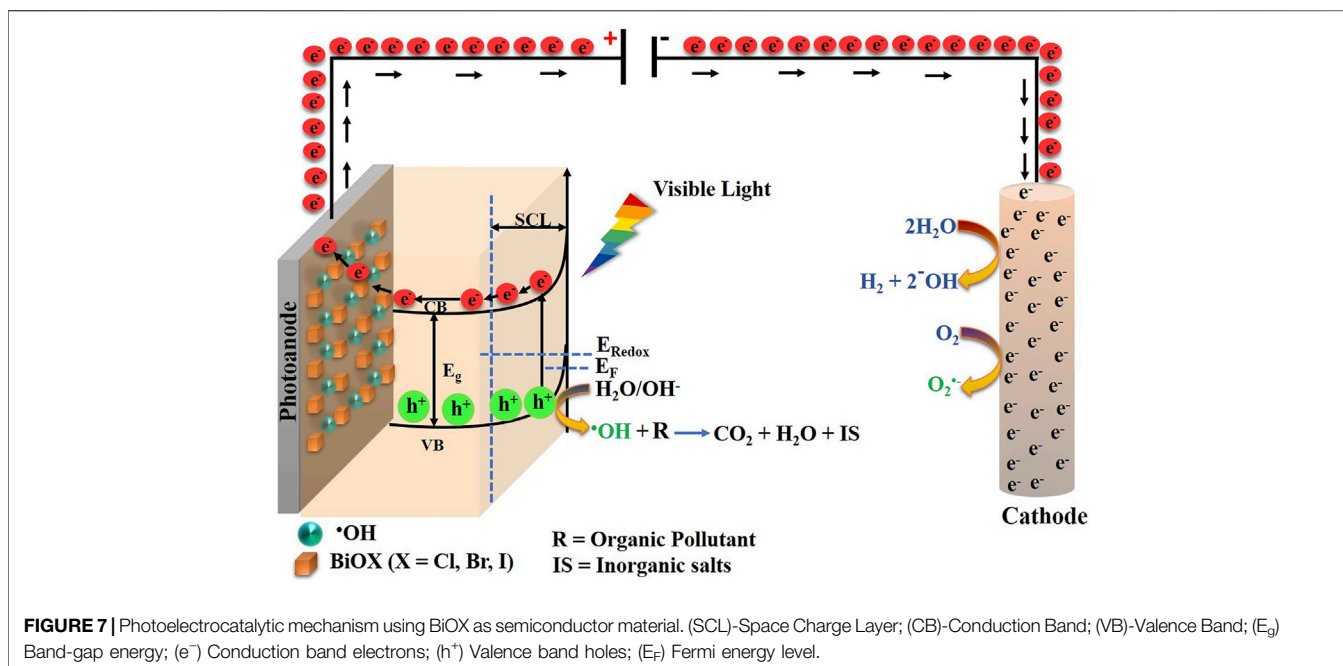
light trapping ability compared to BiOBr. The corresponding band-gap values were 2.85 eV for 0.5S-BiOBr and 3.00 eV for pure BiOBr. In addition, they showed that sulfur doping boosted the formation of oxygen vacancies, which promoted photogenerated charge transfer. Zhang et al. (2020) prepared a Z-type BiOX (X = Cl and Br)-Au-CdS heterojunction by chemical bath deposition. According to the UV-vis DRS spectra, the composite exhibited a slight red shift with respect to pure BiOX, this attributed to the strong interaction between Au and CdS. Additionally, photoluminescence spectroscopy results showed that the heterojunction presented a peak with lower intensity, which translates into a reduction of the recombination rate of the photogenerated e<sub>CB</sub><sup>-</sup>/h<sub>VB</sub><sup>+</sup> pairs.

## 4 BiOX APPLIED IN PHOTOELECTROCATALYSIS

### 4.1 Principles of PEC

PEC constitute an advanced oxidation process (Kusmierek, 2020; Alulema-Pullupaxi et al., 2021a) and is considered an innovative technology, because it is capable of improving photocatalysis process. It has been used to decontaminate aqueous media where organic pollutants predominate in low concentrations and whose degradation or removal is not achieved with traditional processes.

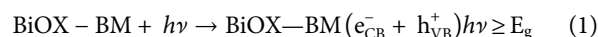




The photoelectrocatalytic mechanism is similar to photocatalysis, except that in PEC, a semiconductor material (photocatalyst) is deposited on the surface of an electrode to form a photoelectrode, whose electronic characteristics determine if it is a photoanode (n-type), where oxidative reactions could be carried out, or a photocathode (p-type), which favors reduction processes (Kusmierek, 2020; Olea, Bueno and Pérez, 2021). In addition, the semiconductor type, solution medium, pH value, nature of the supporting electrolyte, applied current, and light source are some of the factors that affect the efficiency of photoelectrocatalytic processes (Kusmierek, 2020).

Once the photoelectrode of interest has been selected, the photoelectrocatalytic process starts with the photoexcitation of electrons from the valence band (VB) to the conduction band (CB) of the semiconductor material. The energy difference between these two discrete energy levels is called the band-gap (BG or  $E_g$ ). The energy of the photons absorbed by the semiconductor material must be greater or equal to the band-gap energy ( $h\nu \geq E_g$ ), to promote the formation of charge carriers, namely electrons in the conduction band ( $e_{CB}^-$ ) and holes or positive vacancies in the valence band ( $h_{VB}^+$ ). These  $e_{CB}^-/h_{VB}^+$  pairs are important in both photocatalysis and photoelectrocatalytic technologies (Tugaoen et al., 2017; Kusmierek, 2020; Alulema-Pullupaxi et al., 2021a; Alulema-Pullupaxi et al., 2021b; Olea et al., 2021; Sigcha-Pallo et al., 2022). Compared to heterogeneous photocatalysis, PEC also requires an applied bias potential; capable of extracting and transporting electrons through an external circuit, to avoid the recombination of the photogenerated  $e_{CB}^-/h_{VB}^+$  pairs. This phenomenon is a typical disadvantage in photocatalysis (Tugaoen et al., 2017; Vargas et al., 2019; Kusmierek, 2020; Monllor-Satoca et al., 2020). Thus, successful PEC forms  $\bullet\text{OH}$  on the photoanode surface, which are capable of reacting with the

target pollutant molecules and converting them into  $\text{CO}_2$ ,  $\text{H}_2\text{O}$ , and inorganic salts (mineralization) or, in certain cases forming of simpler and readily biodegradable substances (Olea et al., 2021) (Figure 7). The photochemical mechanism is summarized below, with emphasis on the use of BiOX—based material (BiOX—BM) as semiconductor material, which are of interest in this review.



Reaction (3) rarely occurs in photoelectrochemical processes due the electrons of the conduction band are transported *via* an external circuit, by the applied potential (Olea et al., 2021). The generation of holes must occur in a potential range close to the standard redox potential of the  $\bullet\text{OH}$  ( $E^\circ = 2.80$  eV), that is, the energetic position of the conduction band of the semiconducting material is important (Siahrostami et al., 2017; Olea et al., 2021; Wang et al., 2021). BiOX-based materials meet this requirement, so they have been widely used in photo- and photoelectrocatalysis (Xiong et al., 2020; Han, 2021). The electrons concentrated on the cathode surface induce reduction reactions, essentially reduction of  $\text{O}_2$  present in solution to produce superoxide radicals ( $\text{O}_2^{\bullet-}$ , another oxidant).

In addition to the surface reactions that occur in the photoelectrodes, the processes that happen at the interface between the semiconductor and the aqueous medium, specifically between the electrode and the supporting electrolyte (Schottky junction), are also important. This interface is capable of modifying the average electron potential (Fermi energy level), which is closer to the valence band in p-type semiconductors (Alulema-Pullupaxi et al., 2021b). This is the case for most semiconductor materials based on BiOXs (Singh,

Sharma and Khanuja, 2018). Inside the semiconductor material, is the Space Charge Layer (SCL) where a bending of the valence and conduction bands to different energy levels occurs when the material is irradiated with electromagnetic energy, this is called bending band in **Figure 7**. This bending results in a strategy to improve the separation of  $e_{CB}^-/h_{VB}^+$  pairs and decrease the recombination rate, **Figure 7** (Nellist et al., 2016; Kusmierek, 2020; Monllor-Satoca et al., 2020; Peter et al., 2020; Alulema-Pullupaxi et al., 2021a).

Although PEC requires complex systems because of the need for a stable photoelectrode, the application of a bias potential and a light source, it is clear that its advantages outweigh these drawbacks when compared to the degradation process using photocatalysis. In fact, the electrical energy consumed in photoelectrocatalytic degradation is less than that needed for anodic oxidation, which often requires high cell potentials to achieve mineralization (Arotiba et al., 2020).

## 4.2 Environmental Applications of BiOX-Based Materials

Many BiOX-based materials have been developed for environmental remediation applications, and most of these semiconductors have been successful in photocatalytic degradation systems (Huizhong et al., 2008; Chang et al., 2010; Garg et al., 2018). Some authors such as Gao et al. (2021), Wei et al. (2021), and Nava-Núñez et al. (2020) have recently summarized some of the applications of BiOX-based materials in photocatalytic processes. Similarly, Arumugam and Choi (2019) systematically presented the preparation methods and properties of some BiOI-based photocatalysts and their applications in water remediation. Lee et al. (2015) reported the synthesis, characterization, and photocatalytic activity under visible light conditions of some BiOI composites. Further, Liu and Peng (2020) presented the most recent progress in the development of BiOCl photocatalysts.

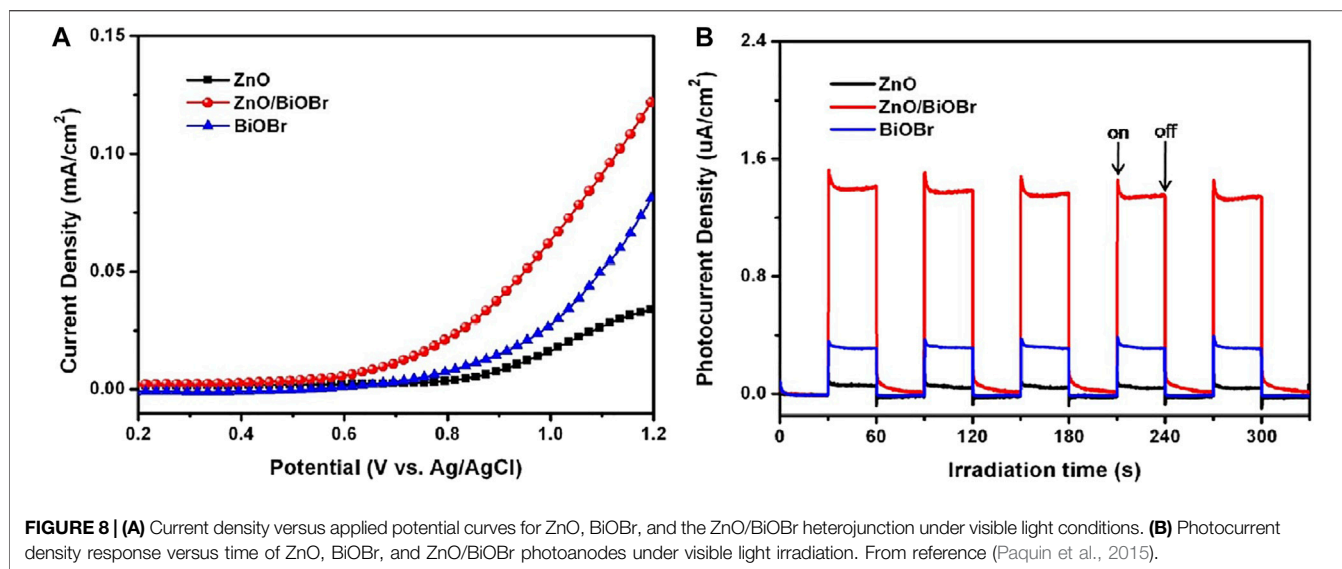
It is important to note that there are few reports of PEC applications focused on environmental remediation. Nevertheless, some research has focused on the development of photoelectrochemical sensors for photoanodic detection of pollutants (Wang et al., 2020). Similarly, some studies have explored the photoelectrochemical behavior of BiOX-based photoanodes (Poznyak and Kulak, 1990; Kwolek and Szaciłowski, 2013; Stephenson et al., 2018) and photocathodes (Bai et al., 2019), under various photoelectrocatalytic reaction conditions. It should be mentioned that just a few studies have discussed theoretical aspects of the electronic and structural characteristics, in addition the optical properties of the synthesized materials. However, a discussion based on computational calculations could be compared to results from experimental applications and subsequently use to predict the behavior of the semiconductors in the electrochemical cell. In the following, we discuss the most recent results in the development of BiOX-based photoelectrocatalysts applied to the decontamination of aqueous media.

### 4.2.1 BiOCl-Based Materials

As mentioned in the above section, one of the most important properties in photocatalytic activity is the band-gap energy. BiOCl has a band-gap approaching that of  $TiO_2$  in its anatase phase ( $\sim 3.20$  eV); therefore, most composites based on this modified first oxide have been produced to improve this feature, as well as its response to visible light. In this regard, Fu et al. (2016) successfully prepared  $TiO_{2-x}/BiOCl$  heterojunctions ( $x$  is the molar ratio of BiOCl to  $TiO_2$ ) and examined the photoelectrocatalytic activity in a three-electrode system.  $TiO_{2-x}/BiOCl$  composites were deposited on an FTO electrode to form the photoanode. Using a 300 W Xe lamp fitted with an AM 1.5 global filter as the light source, they demonstrated that the separation and transport efficiencies of the photogenerated charge carriers were higher for the composite with a 0.3 Bi:Ti molar ratio (TB-0.3) compared to the other photoanodes (TB-0.1 and TB-0.6). The photocurrent of the TB-0.3 photoelectrode increased by the photocurrent density of pure  $TiO_2$  and BiOCl by 10.9 and 22.21 times, respectively. The increased photocurrent density of this new material indicates that it has a high ability to promote the formation and, transfer of and avoid the recombination of  $e_{CB}^-/h_{VB}^+$  pairs (Faraji et al., 2019; Peter et al., 2020). In a more recent study, Mao et al. (2022) prepared a CuO/BiOCl p-n type heterojunction for simultaneous photoelectrochemical detection and photoelectrocatalytic degradation of aflatoxin B1 (AFB1). The modification with CuO nanoparticles improved the responsivity of BiOCl and thus the photocurrent conversion. Using a three-electrode system, they achieved an 81.7% degradation efficiency of a 5.0  $\mu g/L$  solution of AFB 180 min of reaction. This system thus provides a useful method to control AFB1 contamination in food safety areas specifically.

### 4.2.2 BiOBr-Based Materials

Unlike BiOCl materials, bismuth oxybromides have the ability to carry out oxidation-reduction reactions driven by visible light irradiation, because of their slightly narrower band-gap energy ( $\sim 2.7$  eV). However, their fast charge recombination rate and low redox capacity have driven the construction of new BiOBr-based structures (Guo et al., 2021). In this context, Paquin et al. (2015) synthesized BiOBr nanostructures decorated with vertically aligned ZnO nanorods (ZnO/BiOBr). The decoration constitutes a surface modification resulting in a ZnO termination on the BiOBr surface (Li et al., 2021). In this study, a typical system with three electrodes and a 300 W Xe lamp, the photoelectrochemical behavior of this heterojunction was examined in a 0.5 M  $Na_2SO_4$  electrolyte solution; results showed that the optimum content of the raw materials to form BiOBr nanosheets was 0.05 mM [ $KBr + Bi(NO_3)_3$ ] since, at this value, current density reached its maximum. Above this value, aggregates of BiOBr nanoparticles were formed, which led to an increase in the recombination rate of photoexcited  $e_{CB}^-/h_{VB}^+$  pairs. Under a potential sweep from 0.2 to 1.2 V vs. Ag/AgCl a photocurrent response of the ZnO/BiOBr photoanode was identified at approximately 0.64 V, a lower value compared to those of ZnO (0.80 V) and BiOBr (0.79 V) (**Figure 8A**).

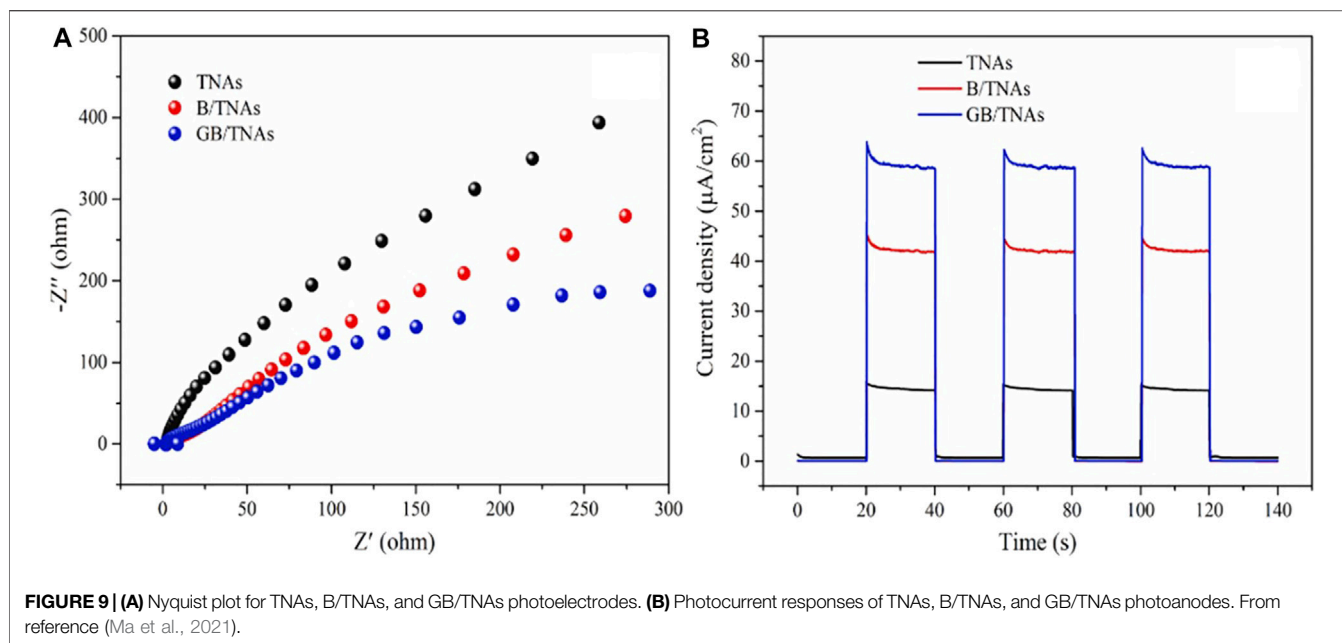


Additionally, the ZnO/BiOBr photoanode had a higher photocurrent density at lower potential values than the ZnO and BiOBr potentials, indicating a decrease in charge recombination in the vicinity of the flat band potential. Conversely, **Figure 8B** shows the photocurrent density response versus time of the prepared photoanodes with an open circuit potential. The increasing and decreasing photocurrent indicates that the photoanode's interface charge transport is very fast, which is attributed to the electron transfer directly from the aligned ZnO nanorods. In addition, the high photocurrent density indicates the effective and rapid separation of charge carriers.

Similarly, Liu et al. (2018) combined the photoelectrochemical degradation of tetracycline using BiOBr as a photoanode and simultaneous CO<sub>2</sub> reduction with a CuO cathode. After applying a potential sweep from 0.6 to 0.8 V vs. Ag/AgCl, 68% of the drug was degraded in 2.5 h of reaction under illumination from a 300 W Xe lamp equipped with a 420 nm cutoff filter, using Pt as a counter electrode. When coupled, CuO as a cathode achieved 80% degradation of the tetracycline at 0.7 V in a photoelectrocatalytic system under the aforementioned conditions. These results demonstrate that there is a significant synergy between the photoelectrocatalytic degradation of tetracycline and CO<sub>2</sub> reduction in the BiOBr/CuO system. In another study, Ling et al. (2020) successfully prepared BiOBr nanosheet arrays (NSAs) using a solvothermal method, and examined their photoelectrocatalytic ability in the degradation of some organic pollutants. Linear scanning voltammetry (LSV) results showed a photocurrent response of the BiOBr NSA-160 photoanode (160 indicates the temperature at which the electrode was prepared) at a bias voltage of 1.4 V under dark conditions. When irradiated with visible light, the photocurrent intensity increased until the bias voltage exceeded 0.9 V. Thus, the increased voltage causes the photoexcited electrons to be transferred to the external circuit, thereby improving the separation efficiency of e<sub>CB</sub><sup>-</sup>/h<sub>VB</sub><sup>+</sup> pairs (Jeon et al., 2018; Wang et al., 2018). The photoelectrocatalytic

activity was evaluated in the degradation of ciprofloxacin (CIP), 91.4% degradation was achieved at the end of 180 min, which was reached once the applied bias voltage was increased up to 0.9 V. The degradation efficiency of CIP increased only slightly once the bias voltage exceeded 0.9 V and decreased when the voltage exceeded 1.8 V. This effect occurs because proper biasing can effectively transfer the photogenerated electrons.

In a more recent study, using an electrodeposition method Ma et al. (2021) synthesized a ternary heterostructure of reduced graphene oxide (rGO)/BiOBr/TiO<sub>2</sub> nanotube arrays (GB/TNAs) for the photoelectrocatalytic degradation of *p*-chloronitrobenzene, the charge transfer kinetics were analyzed *via* electrochemical impedance spectroscopy (EIS). The Nyquist plot in **Figure 9A** shows that the GB/TNAs photoanode has the lowest semicircle signal with respect to the other analyzed photoelectrodes, TNAs (TiO<sub>2</sub> nanotube arrays) and B/TNAs (BiOBr/TiO<sub>2</sub> nanotubes). This indicates that the structure of BiOBr and rGO promoted the transfer of the TNAs charge carriers with reduced resistance. On the other hand, **Figure 9B** shows the photocurrent response over time under cyclic visible light irradiation in an on/off system. The GB/TNAs electrode stabilized at approximately 60 μA/cm<sup>2</sup>, which was 3.75 and 1.43 times higher than that of TNAs and B/TNAs, respectively. This indicates that the GB/TNAs heterojunction has a higher photogenerated charge separation ability. The highest degradation efficiency of a 0.1 mM sample of *p*-chloronitrobenzene was achieved after 6 h of visible light irradiation (300 W Xe lamp), reaching a value of 86.8% using the GB/TNAs photoanode. This value was higher than the efficiencies reported for the B/TNAs and TNAs photoanodes (72.0 and 41.5%, respectively), indicates that introducing of rGO to the semiconductor structure favors the photoelectrocatalytic activity of the system due to its excellent conductivity. Additionally, the pseudo-first order reaction constants corresponding to the degradation process were reported: the constants increased from 0.0037 to 0.0055 min<sup>-1</sup> when a potential sweep from 0 to 1.0 V was applied and decreased



when the potential exceeded 1.5 V. Importantly, photoelectrocatalytic activity was limited by the surface structure of the semiconducting materials serving as photoanodes, in addition to their optical properties and charge separation ability to prevent recombination (Ma et al., 2021). In this context, structural analysis of the photoelectrode surface showed that the BiOBr/TNAs structure was compact, which contributed to better visible light collection and higher charge separation efficiency compared to that of pure TNAs.

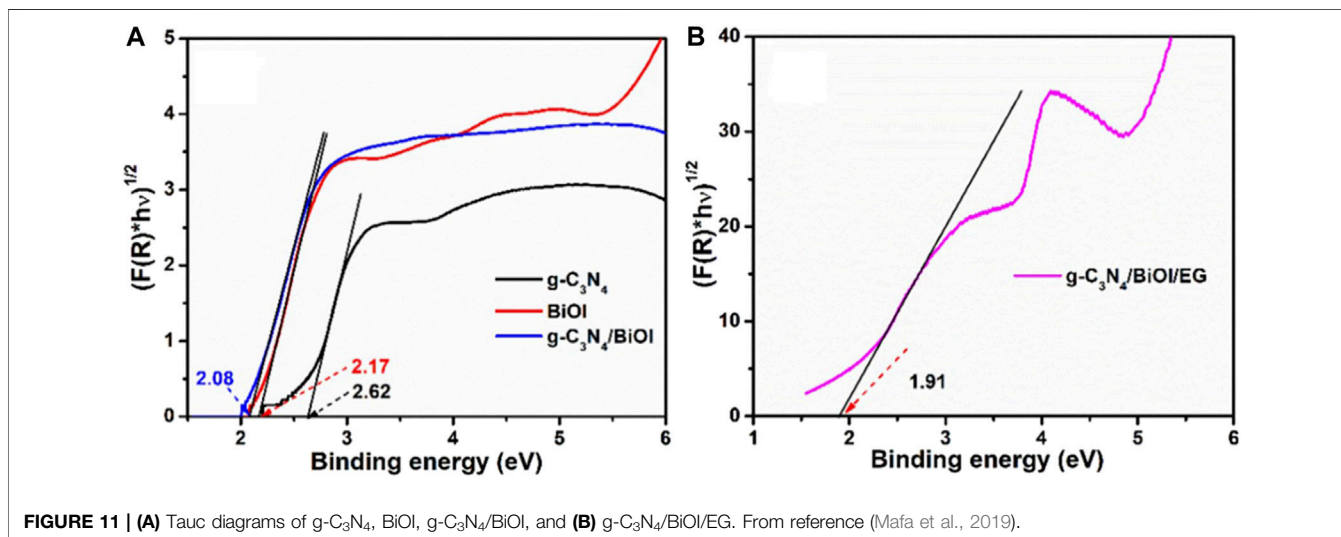
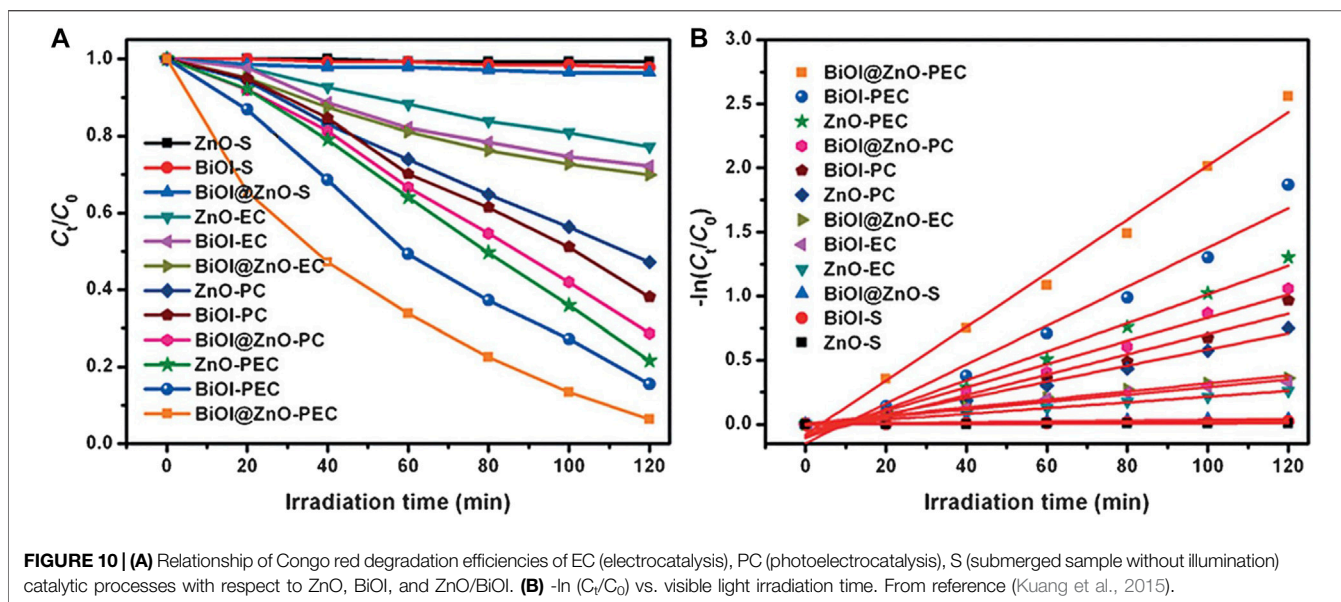
#### 4.2.3 BiOI-Based Materials

BiOI is a p-type semiconductor, with an even narrower bandgap energy than BiOCl and BiOBr (approximately 1.70 eV), and thus, has been considered one of the most promising materials for environmental remediation in both photocatalytic and photoelectrocatalytic systems (Zhang et al., 2008; Hu et al., 2014; Huang et al., 2017). Recently, numerous studies have focused on the design of new BiOI-based materials to treat different pollutants through photocatalytic processes, in which BiOI/TiO<sub>2</sub> heterojunctions (Liao et al., 2021) and Z-type Fe<sub>3</sub>O<sub>4</sub>/BiOCl/BiOI heterostructures (Dang et al., 2022) are included. Additionally, semiconductors based on non-stoichiometric bismuth oxyiodides (Bi<sub>x</sub>O<sub>y</sub>I<sub>z</sub>), also called bismuth-rich bismuth oxyiodides, whose structures exhibit improved stability and whose band structures are more suitable for photocatalytic processes has been reported (Liu and Zhang, 2014; Jin et al., 2017). In addition, multi-walled carbon nanotube/Bi<sub>4</sub>O<sub>5</sub>I<sub>2</sub> (Gao et al., 2022), La<sub>2</sub>Ti<sub>2</sub>O<sub>7</sub>/Bi<sub>5</sub>O<sub>7</sub>I (Zhu et al., 2022), 2D/3D BiOCl/Bi<sub>5</sub>O<sub>7</sub>I heterojunctions (Huang et al., 2022), and Bi<sub>7</sub>O<sub>9</sub>I<sub>3</sub>/g-C<sub>3</sub>N<sub>4</sub>/Bi<sub>3</sub>O<sub>4</sub>Cl (Yuan et al., 2022) heterostructures have been reported.

In the context of PEC, BiOI-based materials have been developed to improve photoanode stability and, charge separation ability and decrease the recombination rate (Guo et al., 2019). In one related study, Kuang et al. (2015)

prepared a p-n type BiOI/ZnO heterojunction using a solvothermal method for the efficient degradation of Congo red (an organic dye). In a three-electrode system and with a 0.5 M Na<sub>2</sub>SO<sub>4</sub> solution, the photoelectrochemical behavior of this composite was investigated. The maximum current density identified at 1.2 V was 0.20 mA/cm<sup>2</sup> which corresponds to a 2.22-fold increase with respect to ZnO and 1.43-fold increase with respect to the BiOI film. After 2 h of reaction, the BiOI/ZnO photoanode had the highest Congo red degradation efficiency, reaching a value of 93.66%. **Figure 10A** shows the comparative relationship of the various degradation processes carried out for this dye. The electrocatalytic and photocatalytic processes reveal a lower degradation efficiency compared to the photoelectrocatalytic process (PEC). Similarly, as shown in **Figure 10B** the kinetic constant of the pseudo-first order reaction is significantly higher in the photoelectrocatalytic process using the BiOI/ZnO material in comparison to the rest of the procedures and materials.

Similarly, Sun et al. (2017) took advantage of the high capacity of CuI as a positive gap carrier and the excellent visible light absorption of BiOI to design a CuI/BiOI heterostructure with exceptional photoelectrocatalytic properties. To demonstrate its degradation capability, Pt nanoparticles were deposited on the composite's surface, and used to degraded methanol and methylene blue (an organic dye) in alkaline solution under dark and visible light. Results showed the optimum amount by weight of Pt nanostructures on the photoanode surface was 10%, above this value, the Pt nanoparticles aggregated with each other, resulting in a high charge density, which decreasing the catalytic ability of the structure. In a typical three-electrode system, using a saturated calomel electrode (SCE) as a reference, 87% of a 10 mg/L solution of methylene blue with Na<sub>2</sub>SO<sub>4</sub> as supporting electrolyte was degraded. Compared to the efficiencies



obtained using pure BiOI and CuI (68 and 8%, respectively), the improvement of the photoelectrocatalytic activity of BiOI is attributed to the introduction of CuI as a promoter of charge separation. Some of the most relevant applications reported thus far focus on the photoelectrocatalytic decomposition of active pharmaceutical ingredients. In this field, Mafa et al. (2019) synthesized a photoanode based on a p-n  $g-C_3N_4/BiOI/EG$  type heterojunction (EG: exfoliated graphite), for the photoelectrocatalytic degradation of sulfamethoxazole (an antibiotic); an approximate removal efficiency of 88% was achieved at a maximum current density of  $5 \text{ mA/cm}^2$  and a pH of 6.23. They also reported the estimated band-gap energy of the synthesized materials. Figures 11A,B show the Tauc plots obtained for the materials, which demonstrate the decreased band-gap energy of the  $g-C_3N_4/BiOI/EG$  composite ( $\sim 1.91 \text{ eV}$ ).

In another study, Liu et al. (2019) highlighted the stability of the electrodeposition-prepared  $BiOI/BiPO_4/FTO$  photoanode in the photoelectrocatalytic degradation of tetracycline in an aqueous medium. XRD results before and after the cycling photoelectrocatalytic tests showed that the  $BiOI/BiPO_4/FTO$  photoelectrode had excellent stability to degrade this pharmaceutical pollutant. The degradation rate was not affected after four 16 h degradation cycles. Thus, it can be considered a material with excellent characteristics for decontaminating aqueous media in photoelectrocatalytic systems.

In addition to requiring a stable photoanode with good effectiveness against visible light, photoelectrocatalytic degradation efficiency is further limited by the reaction pathway the pollutant molecule follows to mineralization or,

**TABLE 1** | Characteristics of BiOX-based materials in the photoelectrocatalytic degradation of some organic pollutants.

Semiconductor material (photoanode)	Synthesis/Preparation method	Pollutant type	Pollutant	Experimental conditions	Degradation efficiency (%)	References
g-C <sub>3</sub> N <sub>4</sub> /BiOI/EG	Ultrasound assisted	Antibiotic	Sulfamethoxazole (SMX)	CE: Pt wire RE: Ag/AgCl (3 M KCl) t: 30 min; pH: 6.23 CD: 5 mA/cm <sup>2</sup> ; HAL-320 (Xe lamp 300-W)	88.0	Mafa et al. (2019)
CuI/BiOI	Hydrothermal-ultrasound Assisted	Organic dye	Methylene blue (MB)	CE: Pt wire; RE: SCE t: 2 h; V: 20 ml C <sub>0</sub> : 10 mg/L Xe lamp 300-W	87.0	Sun et al. (2017)
ZnO/BiOBr	Solvothermal	Organic dye	Rhodamine B (RhB)	CE: Pt sheet (1 cm <sup>2</sup> ) RE: Ag/AgCl t: 100 min; V: 50 ml; C: 0.1 mM; 0.1 M Na <sub>2</sub> SO <sub>4</sub> ; Xe lamp 300-W	95.4	Paquin et al. (2015)
BiOBr/TiO <sub>2</sub> (B/TNAs)	Adsorption and successive ionic layer reaction (SILAR)	Phenolic derivate	p-chloronitrobenzene (p-CNB)	CE: Pt foil, t: 6 h; V: 50 ml; C: 0.1 mM	72.0 ± 3.2	Ma et al. (2021)
Graphene oxide/BiOBr/TiO <sub>2</sub> (GB/TNAs)	Electrodeposition				86.8 ± 3.6	Ma et al. (2021)
ITO glass/BiOBr NSA-160	Solvothermal	Antibiotic	Ciprofloxacin (CIP)	CE: Pt plate RE: Ag/AgCl (3 M KCl) t: 180 min; C: 15 mg/L; 0.1 M Na <sub>2</sub> SO <sub>4</sub> ; CD: 69 μAcm <sup>-2</sup> Xe lamp 500-W	91.4	Ling, Dai and Zhou, (2020)
		Organic dye	Rhodamine B (RhB)	CE: Pt plate RE: Ag/AgCl (3 M KCl) t: 90 min; Xe lamp 500-W	94.3	Ling, Dai and Zhou, (2020)
		Antibiotic	Tetracycline	CE: Pt plate RE: Ag/AgCl (3 M KCl) t: 180 min; C: 15 mg/L; 0.1 M Na <sub>2</sub> SO <sub>4</sub> ; Xe lamp 500-W	93.2	Ling, Dai and Zhou, (2020)
		Organic derivate	Bisphenol A	CE: Pt plate RE: Ag/AgCl (3 M KCl) t: 180 min; C: 15 mg/L; 0.1 M Na <sub>2</sub> SO <sub>4</sub> ; Xe lamp 500-W	67.5	Ling, Dai and Zhou, (2020)
		Analgesic	Acetaminophen	CE: Pt foil RE: Ag/AgCl (3 M KCl) t: 2 h; C: 10 mg/L; 0.1 M Na <sub>2</sub> SO <sub>4</sub> ; V: 50 ml Xe lamp 100-W	68.0	Orimolade et al. (2019)
FTO/BiVO <sub>4</sub> /BiOI	Electrodeposition	Antibiotic	Ciprofloxacin (CIP)	CE: Pt foil RE: Ag/AgCl (3 M KCl) t: 2 h; C: 10 mg/L; 0.1 M Na <sub>2</sub> SO <sub>4</sub> ; V: 50 ml Xe lamp 100-W	62.0	Orimolade et al. (2019)
		Organic dye	Orange (II)	CE: Pt foil RE: Ag/AgCl (3 M KCl) t: 2 h; 0.1 M Na <sub>2</sub> SO <sub>4</sub> Xe lamp 100-W	85.0	Orimolade et al. (2019)
Bi <sub>2</sub> O <sub>3</sub> -BiOI	Simple immersion	Organic derivate	Phenol	CE: Ti; pH: 6.2 V: 50 ml; C: 10 mg/L; 0.2 M Na <sub>2</sub> SO <sub>4</sub> Xe lamp 500-W	—	Cong et al. (2017)
CuO/BiOCl/ITO	<i>In-situ</i> growth	Organic derivate	Aflatoxin B1 (AFB1)	CE: Pt wire RE: Ag/AgCl saturado t: 180 min; C: 5 μg/L PEAC 200 A PEC reaction instrument	81.7	Mao et al. (2022)
BiOBr/FTO	Solvothermal	Antibiotic	Tetracycline	CE: CuO RE: Ag/AgCl t: 2.5 h; V: 80 ml; C: 10 ppm, 0.1 M Na <sub>2</sub> SO <sub>4</sub> ; 0.1 M KHCO <sub>3</sub> Xe lamp 300-W	80.0	Liu et al. (2018)
BiOI/BiPO <sub>4</sub> /FTO	Electrodeposition	Antibiotic	Tetracycline	CE: Pt wire RE: SCE V: 100 ml; C: 10 ppm 0.1 M Na <sub>2</sub> SO <sub>4</sub> Xe lamp 500-W	77.0	Liu et al. (2019)
FTO/TiO <sub>2</sub> -/BiOCl	Ultrasound Assisted	Organic dye	Rhodamine B (RhB)	CE: Pt wire RE: Ag/AgCl 0.5 M Na <sub>2</sub> SO <sub>4</sub> Xe lamp 300-W	—	Fu et al. (2016)
FTO/BiOI/ZnO	Electrodeposition	Organic dye	Congo red (CR)	CE: Pt sheet RE: Ag/AgCl t: 2 h V: 60 ml; C: 0.1 mM 0.1 M Na <sub>2</sub> SO <sub>4</sub> Xe lamp 300-W	93.6	Kuang et al. (2015)
BiOI/GH/FTO	Electrodeposition	Organic derivate	Phenol (Ph-OH)	CE: Pt wire RE: SCE t: 5 h; C: 5 ppm 0.1 M Na <sub>2</sub> SO <sub>4</sub> Xe lamp 500 mW/cm <sup>2</sup>	83.0	Chen et al. (2018)

CE, Counter electrode; RE, Reference electrode;

in other cases, to simpler substances (Yang et al., 2018; Ahmad et al., 2021). Orimolade et al. (2019) reported degradation efficiencies of acetaminophen (68%), CIP (62%), and orange II (85%) for a photoelectrocatalytic system using a BiVO<sub>4</sub>/BiOI composite as the photoanode, they also determined the charge transfer mechanism in the photoelectrochemical system. During

the formation of the internal electric field when BiVO<sub>4</sub> and BiOI are in contact, electrons are able to migrate until the Fermi energy level are equivalent between the two semiconducting materials. After this process, the band energy edges of the modified bismuth oxides are adjusted producing a potential difference between these two materials; that is, the electrons accumulated in the

conduction band of BiOI migrate towards the conduction band of BiOV<sub>4</sub> and likewise the positive vacancies (photogenerated holes) (Orimolade et al., 2019). The migration direction of the photogenerated electrons and holes into the conduction and valence bands depends on the type of heterojunction formed between the composing semiconductors (Y. Li et al., 2021). In this way, the composite achieves a better charge separation and thus a higher degradation efficiency compared to individual materials. This is because, there are more holes able to oxidize the contaminant molecules or produce hydroxyl radicals (strong oxidants) when they react with the water, and superoxide radicals when the electrons on the cathode surface reduce the oxygen in the solution (Younis et al., 2020; Garcia-Segura et al., 2021).

Definitely, **Table 1** summarizes the most recent applications of BiOX-based photoanodes prepared by various synthesis methods, intended for the degradation of organic pollutants in aqueous media. It also includes the experimental conditions of the photoelectrochemical systems used for the visible light-driven degradation reactions and the reported degradation efficiencies for some organic pollutants, particularly highlighting active pharmaceutical ingredients, including antibiotics and analgesics, organic dyes, and some phenol derivatives.

## 5 CONCLUSION AND FUTURE CHALLENGES

In response to the need to develop new economical, efficient, and environmentally friendly technologies for pollutant degradation interest has grown in developing innovative, low-cost semiconductor materials able to degrade pollutants present in different ecosystems at low concentrations. The present review has focused on analyzing the most recent research on the properties of BiOX (X = Cl, Br, and I)—based materials and their ability to degrade organic compounds in aqueous media by means of PEC; this relatively new technology, which is undergoing constant innovation, enhances the characteristics of heterogeneous photocatalysis by applying advanced electrochemical oxidation. In addition, the optimal experimental conditions of each photoelectrocatalytic system and the degradation efficiencies for some organic pollutants were presented. The optical and structural properties that demonstrate the high capacity of these oxides to capture and harness visible light

energy to promote important oxidation-reduction reactions in a photoelectrochemical process were also addressed. Finally, the advantages and disadvantages of the photoelectrocatalytic mechanism were discussed, with an emphasis on the use of BiOX-based materials as photoanodes.

The present review highlights the countless challenges and possibilities for improving the characteristics and properties of BiOX-based materials, and other semiconductors. It also focuses on the systematization of new technologies that take advantage of the performance of these semiconductors, for example by directly utilizing solar energy instead of light sources simulating such energy, to make these procedures not only more efficient but also environmentally and economically advantageous. Therefore, great efforts must be made to limit the economic and energy costs in the design and construction of materials and technologies based on advanced electrochemical processes.

Another interesting challenge with BiOX-based photocatalysts that only a few studies have reported with is the optimization of photochemical and photoelectrochemical processes by coupling new systems—that is, two or more processes occurring simultaneously in the electrochemical cell—to gain complete control of the kinetics, thermodynamics and efficiency of the processes. Ultimately, all efforts to improve existing or generate new and innovative technologies should center on readying these systems to be engineered and introducing these technologies and materials in real water treatment plans that prioritize pollutant removal to have an actual impact on the environment.

## AUTHOR CONTRIBUTIONS

Conceptualization, GC-C, PE-M, and PA-P; methodology, PE-M, GC-C; investigation, GC-C, PE-M, PA-P, JRM, and MV-G; writing—original draft preparation, GC-C, PE-M, and PA-P; writing—review and editing, GC-C, PE-M, PA-P, JRM, and MV-G; supervision PE-M; project administration, PE-M. All authors have read and agreed to the published version of the manuscript.

## ACKNOWLEDGMENTS

The authors thank the Office of Research at the Pontificia Universidad Católica del Ecuador for funding the project and the Universidad Central Del Ecuador.

## REFERENCES

- Ahmad, I., Shukrullah, S., Yasin Naz, M., Ullah, S., and Ali Assiri, M. (2022). Designing and Modification of Bismuth Oxyhalides BiOX (X = Cl, Br and I) Photocatalysts for Improved Photocatalytic Performance. *J. Industrial Eng. Chem.* 105, 1–33. doi:10.1016/j.jiec.2021.09.030
- Alulema-Pullupaxi, P., Espinoza-Montero, P. J., Sigcha-Pallo, C., Vargas, R., Fernández, L., Peralta-Hernández, J. M., et al. (2021a). Fundamentals and Applications of Photoelectrocatalysis as an Efficient Process to Remove Pollutants from Water: A Review. *Chemosphere* 281, 130821. doi:10.1016/j.chemosphere.2021.130821
- Alulema-Pullupaxi, P., Fernández, L., Debut, A., Santacruz, C. P., Villacis, W., Fierro, C., et al. (2021b). Photoelectrocatalytic Degradation of Glyphosate on Titanium Dioxide Synthesized by Sol-Gel/spin-Coating on Boron Doped Diamond (TiO<sub>2</sub>/BDD) as a Photoanode. *Chemosphere* 278, 130488. doi:10.1016/j.chemosphere.2021.130488
- Arotiba, O. A., Orimolade, B. O., and Koiki, B. A. (2020). Visible Light-Driven Photoelectrocatalytic Semiconductor Heterojunction Anodes for Water Treatment Applications. *Curr. Opin. Electrochem.* 22, 25–34. doi:10.1016/j.coelec.2020.03.018
- Arumugam, M., and Choi, M. Y. (2020). Recent Progress on Bismuth Oxyiodide (BiOI) Photocatalyst for Environmental Remediation. *J. Industrial Eng. Chem.* 81, 237–268. doi:10.1016/j.jiec.2019.09.013

- Bagheri, S., Termehousefi, A., and Do, T.-O. (2017). Photocatalytic Pathway toward Degradation of Environmental Pharmaceutical Pollutants: Structure, Kinetics and Mechanism Approach. *Catal. Sci. Technol.* 7, 4548–4569. doi:10.1039/C7CY00468K
- Bai, S., Li, X., Kong, Q., Long, R., Wang, C., Jiang, J., et al. (2015). Toward Enhanced Photocatalytic Oxygen Evolution: Synergetic Utilization of Plasmonic Effect and Schottky Junction via Interfacial Facet Selection. *Adv. Mat.* 27 (22), 3444–3452. doi:10.1002/adma.201501200
- Bai, Y., Bai, H., Qu, K., Wang, F., Guan, P., Xu, D., et al. (2019). *In-situ* Approach to Fabricate BiOI Photocathode with Oxygen Vacancies: Understanding the N<sub>2</sub> Reduced Behavior in Photoelectrochemical System. *Chem. Eng. J.* 362, 349–356. doi:10.1016/J.CEJ.2019.01.051
- Barhoumi, M., and Said, M. (2021). Electronic and Optical Properties of Bismuth Oxyhalides from Ab Initio Calculations. *Mater. Sci. Eng. B* 264, 114921. doi:10.1016/j.mseb.2020.114921
- Cao, F., Wang, Y., Wang, J., Lv, X., Liu, D., Ren, J., et al. (2018). Oxygen Vacancy Induced Superior Visible-Light-Driven Photodegradation Pollutant Performance in BiOCl Microflowers. *New J. Chem.* 42 (5), 3614–3618. doi:10.1039/c7nj04041e
- Chang, X., Huang, J., Cheng, C., Sui, Q., Sha, W., Ji, G., et al. (2010). BiOX (X = Cl, Br, I) Photocatalysts Prepared Using NaBiO<sub>3</sub> as the Bi Source: Characterization and Catalytic Performance. *Catal. Commun.* 11 (5), 460–464. doi:10.1016/j.catcom.2009.11.023
- Chen, D., Yang, J., Zhu, Y., Zhang, Y., and Zhu, Y. (2018). Fabrication of BiOI/graphene Hydrogel/FTO Photoelectrode with 3D Porous Architecture for the Enhanced Photoelectrocatalytic Performance. *Appl. Catal. B Environ.* 233, 202–212. doi:10.1016/j.apcatb.2018.04.004
- Cong, Y., Ji, Y., Ge, Y., Jin, H., Zhang, Y., and Wang, Q. (2017). Fabrication of 3D Bi<sub>2</sub>O<sub>3</sub>-BiOI Heterojunction by a Simple Dipping Method: Highly Enhanced Visible-Light Photoelectrocatalytic Activity. *Chem. Eng. J.* 307, 572–582. doi:10.1016/j.cej.2016.08.114
- Cui, Z., Song, H., Ge, S., He, W., and Liu, Y. (2019). Fabrication of BiOCl/BiOBr Hybrid Nanosheets with Enhanced Superoxide Radical Dominating Visible Light Driven Photocatalytic Activity. *Appl. Surf. Sci.* 467–468, 505–513. doi:10.1016/j.apsusc.2018.10.181
- Dai, W.-W., and Zhao, Z.-Y. (2017). Structural and Electronic Properties of Low-Index Stoichiometric BiOI Surfaces. *Mater. Chem. Phys.* 193, 164–176. doi:10.1016/j.matchemphys.2017.02.017
- Dang, J., Guo, J., Wang, L., Guo, F., Shi, W., Li, Y., et al. (2022). Construction of Z-Scheme Fe<sub>3</sub>O<sub>4</sub>/BiOCl/BiOI Heterojunction with Superior Recyclability for Improved Photocatalytic Activity towards Tetracycline Degradation. *J. Alloys Compd.* 893, 162251. doi:10.1016/J.JALLCOM.2021.162251
- Faraji, M., Yousefi, M., Yousefzadeh, S., Zirak, M., Naseri, N., Jeon, T. H., et al. (2019). Two-dimensional Materials in Semiconductor Photoelectrocatalytic Systems for Water Splitting. *Energy Environ. Sci.* 12 (1), 59–95. doi:10.1039/c8ee00886h
- Fu, H. R., et al. (2016). Enhanced Photocatalytic and Photoelectrochemical Activities of Reduced TiO<sub>2-x</sub>/BiOCl. Available at: <http://www.elsevier.com/open-access/userlicense/1.0/> (Accessed October 27, 2021).
- Ganose, A. M., Cuff, M., Butler, K. T., Walsh, A., and Scanlon, D. O. (2016). Interplay of Orbital and Relativistic Effects in Bismuth Oxyhalides: BiOF, BiOCl, BiOBr, and BiOI. *Chem. Mat.* 28 (7), 1980–1984. doi:10.1021/acs.chemmater.6b00349
- Gao, B., Zhang, J.-R., Chen, L., Guo, J., Shen, S., Au, C.-T., et al. (2019). Density Functional Theory Calculation on Two-Dimensional MoS<sub>2</sub>/BiOX (X = Cl, Br, I) Van Der Waals Heterostructures For Photocatalytic Action. *Appl. Surf. Sci.* 492 (May), 157–165. doi:10.1016/j.apsusc.2019.06.201
- Gao, P., Li, Z., Feng, L., Liu, Y., Du, Z., and Zhang, L. (2022). Construction of Novel MWCNTs/Bi<sub>4</sub>O<sub>5</sub>I<sub>2</sub> Nanosheets with Enhanced Adsorption and Photocatalytic Performance for the Degradation of Tetracycline: Efficiency, Mechanism and Regeneration. *Chem. Eng. J.* 429, 132398. doi:10.1016/j.cej.2021.132398
- Gao, P., Yang, Y., Yin, Z., Kang, F., Fan, W., Sheng, J., et al. (2021). A Critical Review on Bismuth Oxyhalide Based Photocatalysis for Pharmaceutical Active Compounds Degradation: Modifications, Reactive Sites, and Challenges. *J. Hazard. Mater.* 412, 412125186. doi:10.1016/j.jhazmat.2021.125186
- Garcia-Ivars, J., Martella, L., Massella, M., Carbonell-Alcaina, C., Alcaina-Miranda, M.-I., and Iborra-Clar, M.-I. (2017). Nanofiltration as Tertiary Treatment Method for Removing Trace Pharmaceutically Active Compounds in Wastewater from Wastewater Treatment Plants. *Water Res.* 125, 360–373. doi:10.1016/j.watres.2017.08.070
- Garcia-Segura, S., Arotiba, O. A., and Brillas, E. (2021). The Pathway towards Photoelectrocatalytic Water Disinfection: Review and Prospects of a Powerful Sustainable Tool. *Catalysts* 2021Vol. 1111 (8), 921921. doi:10.3390/CATAL11080921
- Garcia-Segura, S., Qu, X., Alvarez, P. J. J., Chaplin, B. P., Chen, W., Crittenden, J. C., et al. (2020). Opportunities for Nanotechnology to Enhance Electrochemical Treatment of Pollutants in Potable Water and Industrial Wastewater - a Perspective. *Environ. Sci. Nano* 7 (8), 2178–2194. doi:10.1039/d0en00194e
- Garg, S., Yadav, M., Chandra, A., and Hernadi, K. (2019). A Review on BiOX (X = Cl, Br and I) Nano-/Microstructures for Their Photocatalytic Applications. *J. Nanosci. Nanotechnol.* 19 (1), 280–294. doi:10.1166/jnn.2019.15771
- Guo, J., Li, X., Liang, J., Yuan, X., Jiang, L., Yu, H., et al. (2021). Fabrication and Regulation of Vacancy-Mediated Bismuth Oxyhalide towards Photocatalytic Application: Development Status and Tendency. *Coord. Chem. Rev.* 443, 214033. doi:10.1016/j.ccr.2021.214033
- Guo, M., Zhou, Z., Yan, S., Zhou, P., Miao, F., Liang, S., et al. (2020). Bi<sub>2</sub>WO<sub>6</sub>-BiOCl Heterostructure with Enhanced Photocatalytic Activity for Efficient Degradation of Oxytetracycline. *Sci. Rep.* 10 (1), 11–13. doi:10.1038/s41598-020-75003-x
- Guo, Y., Shi, W., Zhu, Y., Xu, Y., and Cui, F. (2020). Enhanced Photoactivity and Oxidizing Ability Simultaneously via Internal Electric Field and Valence Band Position by Crystal Structure of Bismuth Oxyiodide. *Appl. Catal. B Environ.* 262, 118262. doi:10.1016/j.apcatb.2019.118262
- Han, Q. (2021). Advances in Preparation Methods of Bismuth-Based Photocatalysts. *Chem. Eng. J.* 414 (September), 127877. doi:10.1016/j.cej.2020.127877
- Hassani, A., Krishnan, S., Scaria, J., Eghbali, P., and Nidheesh, P. V. (2021). Z-Scheme Photocatalysts for Visible-Light-Driven Pollutants Degradation: A Review on Recent Advancements. *Curr. Opin. Solid State Mater. Sci.* 25 (5), 100941. doi:10.1016/j.cossms.2021.100941
- Hou, J., Jiang, K., Shen, M., Wei, R., Wu, X., Idrees, F., et al. (2017). Micro and Nano Hierarchical Structures of BiOI/activated Carbon for Efficient Visible-Light-Photocatalytic Reactions. *Sci. Rep.* 7 (1), 1–10. doi:10.1038/s41598-017-12266-x
- Hu, J., Weng, S., Zheng, Z., Pei, Z., Huang, M., and Liu, P. (2014). Solvents Mediated-Synthesis of BiOI Photocatalysts with Tunable Morphologies and Their Visible-Light Driven Photocatalytic Performances in Removing of Arsenic from Water. *J. Hazard. Mater.* 264, 293–302. doi:10.1016/j.jhazmat.2013.11.027
- Huang, H., Xiao, K., Zhang, T., Dong, F., and Zhang, Y. (2017). Rational Design on 3D Hierarchical Bismuth Oxyiodides via *In Situ* Self-Template Phase Transformation and Phase-Junction Construction for Optimizing Photocatalysis against Diverse Contaminants. *Appl. Catal. B Environ.* 203, 879–888. doi:10.1016/j.apcatb.2016.10.082
- Huang, W., Xiao, X., Lu, M., and Xiao, Y. (2022). *In-situ* Fabrication of Novel BiOCl/Bi<sub>5</sub>O<sub>7</sub>I 2D/3D Heterostructures with Enhanced Photocatalytic Activity. *J. Alloys Compd.* 895, 162669. doi:10.1016/J.JALLCOM.2021.162669
- Huang, Y., Li, H., Balogun, M.-S., Liu, W., Tong, Y., Lu, X., et al. (2014). Oxygen Vacancy Induced Bismuth Oxyiodide with Remarkably Increased Visible-Light Absorption and Superior Photocatalytic Performance. *ACS Appl. Mat. Interfaces* 6 (24), 22920–22927. doi:10.1021/am507641k
- Huizhong, A. N., et al. (2008). Photocatalytic Properties of BiOX (X = Cl, Br, and I). *RARE Met.* 27 (3), 243.
- Jeon, T. H., Koo, M. S., Kim, H., and Choi, W. (2018). Dual-Functional Photocatalytic and Photoelectrocatalytic Systems for Energy- and Resource-Recovering Water Treatment. *ACS Catal.* 8 (12), 11542–11563. doi:10.1021/acscatal.8b03521
- Jin, X., Ye, L., Xie, H., and Chen, G. (2017). Bismuth-rich Bismuth Oxyhalides for Environmental and Energy Photocatalysis. *Coord. Chem. Rev.* 349, 84–101. doi:10.1016/j.ccr.2017.08.010
- Kuang, P.-Y., Ran, J.-R., Liu, Z.-Q., Wang, H.-J., Li, N., Su, Y.-Z., et al. (2015). Enhanced Photoelectrocatalytic Activity of BiOI Nanoplate-Zinc Oxide



- Nanorod P-N Heterojunction. *Chem. Eur. J.* 21 (43), 15360–15368. doi:10.1002/chem.201501183
- Kumar, R., Raizada, P., Verma, N., Hosseini-Bandegharai, A., Thakur, V. K., Le, Q. V., et al. (2021). Recent Advances on Water Disinfection Using Bismuth Based Modified Photocatalysts: Strategies and Challenges. *J. Clean. Prod.* 297, 126617. doi:10.1016/j.jclepro.2021.126617
- Kusmirek, E. (2020). Semiconductor Electrode Materials Applied in Photoelectrocatalytic Wastewater Treatment-An Overview. *Catalysts* 10 (4), 439–449. doi:10.3390/catal10040439
- Kwolek, P., and Szacilowski, K. (2013). Photoelectrochemistry of N-type Bismuth Oxide. *Electrochimica Acta* 104, 448–453. doi:10.1016/j.electacta.2012.10.001
- Lee, A.-H., Wang, Y.-C., and Chen, C.-C. (2019). Composite Photocatalyst, Tetragonal Lead Bismuth Oxide/bismuth Oxide/Graphitic Carbon Nitride: Synthesis, Characterization, and Photocatalytic Activity. *J. Colloid Interface Sci.* 533, 319–332. doi:10.1016/j.jcis.2018.08.008
- Lee, W. W., Lu, C.-S., Chuang, C.-W., Chen, Y.-J., Fu, J.-Y., Siao, C.-W., et al. (2015). Synthesis of Bismuth Oxidides and Their Composites: Characterization, Photocatalytic Activity, and Degradation Mechanisms. *RSC Adv.* 5 (30), 23450–23463. doi:10.1039/c4ra15072d
- Li, G., Wang, X., Zhang, L., and Zhu, C. (2021). Electronic Structures and Optical Properties of BiOBr/BiOI Heterojunction with an Oxygen Vacancy. *Chem. Phys.* 549 (June), 111264. doi:10.1016/j.chemphys.2021.111264
- Li, M., Li, J., Guo, C., and Zhang, L. (2018). Doping Bismuth Oxyhalides with Indium: A DFT Calculations on Tuning Electronic and Optical Properties. *Chem. Phys. Lett.* 705, 31–37. doi:10.1016/j.cplett.2018.05.053
- Li, Y., Luo, K., Tao, R., Wang, Z., Chen, D., and Shao, Z. (2020). A New Concept and Strategy for Photovoltaic and Thermoelectric Power Generation Based on Anisotropic Crystal Facet Unit. *Adv. Funct. Mat.* 30 (28), 2002606–2002609. doi:10.1002/adfm.202002606
- Li, S. S., Shan, S., Chen, S., Li, H., Li, Z., Liang, Y., et al. (2021). Photocatalytic Degradation of Hazardous Organic Pollutants in Water by Fe-MOFs and Their Composites: A Review. *J. Environ. Chem. Eng.* 9, 105967. doi:10.1016/j.jece.2021.105967
- Li, Y. Y., Jiang, H., Wang, X., Hong, X., and Liang, B. (2021). Recent Advances in Bismuth Oxyhalide Photocatalysts for Degradation of Organic Pollutants in Wastewater. *RSC Adv.* 11 (43), 26855–26875. doi:10.1039/d1ra05796k
- Liao, X., Li, T.-T., Ren, H.-T., Zhang, X., Shen, B., Lin, J.-H., et al. (2022). Construction of BiOI/TiO<sub>2</sub> Flexible and Hierarchical S-Scheme Heterojunction Nanofibers Membranes for Visible-Light-Driven Photocatalytic Pollutants Degradation. *Sci. Total Environ.* 806, 150698. doi:10.1016/j.scitotenv.2021.150698
- Lin, Y.-Y., Hung, J.-T., Chou, Y.-C., Shen, S.-J., Wu, W.-T., Liu, F.-Y., et al. (2022). Synthesis of Bismuth Oxybromochloroiodide/graphitic Carbon Nitride Quaternary Composites (BiO<sub>m</sub>Cl<sub>n</sub>/BiO<sub>m</sub>Br<sub>n</sub>/BiO<sub>p</sub>I<sub>q</sub>/g-C<sub>3</sub>N<sub>4</sub>) Enhances Visible-Light-Driven Photocatalytic Activity. *Catal. Commun.* 163, 106418. doi:10.1016/j.cattcom.2022.106418
- Ling, Y., Dai, Y., and Zhou, J. (2020). Fabrication and High Photoelectrocatalytic Activity of Scaly BiOBr Nanosheet Arrays. *J. Colloid Interface Sci.* 578, 326–337. doi:10.1016/j.jcis.2020.05.111
- Liu, C., and Zhang, D. (2014). Large-scale One-Dimensional Bi<sub>x</sub>O<sub>y</sub>I<sub>z</sub> Nanostructures: Synthesis, Characterization, and Photocatalytic Applications. *Appl. Phys. A* 118118 (3), 3913–3922. doi:10.1007/S00339-014-8811-7
- Liu, S.-S., Xing, Q.-J., Chen, Y., Zhu, M., Jiang, X.-H., Wu, S.-H., et al. (2018). Photoelectrochemical Degradation of Organic Pollutants Using BiOBr Anode Coupled with Simultaneous CO<sub>2</sub> Reduction to Liquid Fuels via CuO Cathode. *ACS Sustain. Chem. Eng.* 7, 1250–1259. doi:10.1021/acssuschemeng.8b04917
- Liu, S., Zhao, M., He, Z., Zhong, Y., Ding, H., and Chen, D. (2019). Preparation of a P-N Heterojunction 2D BiOI nanosheet/1DBiPO<sub>4</sub> Nanorod Composite Electrode for Enhanced Visible Light Photoelectrocatalysis. *Chin. J. Catal.* 40, 446–457. doi:10.1016/S1872-2067(18)63186-9
- Liu, W.-W., and Peng, R.-F. (2020). Recent Advances of Bismuth Oxichloride Photocatalytic Material: Property, Preparation and Performance Enhancement. *J. Electron. Sci. Technol.* 18 (2), 100020–100137. doi:10.1016/j.jnlest.2020.100020
- Liu, Y., Hu, Z., and Yu, J. C. (2021). Photocatalytic Degradation of Ibuprofen on S-Doped BiOBr. *Chemosphere* 278, 130376. doi:10.1016/j.chemosphere.2021.130376
- Ma, B., Xin, S., Ma, X., Zhang, C., and Gao, M. (2021). Preparation of Ternary Reduced Graphene oxide/BiOBr/TiO<sub>2</sub> Nanotube Arrays for Photoelectrocatalytic Degradation of P-Chloronitrobenzene under Visible Light Irradiation. *Appl. Surf. Sci.* 551 (238), 149480. doi:10.1016/j.apsusc.2021.149480
- Mafa, P. J., Kuvarega, A. T., Mamba, B. B., and Ntsendwana, B. (2019). Photoelectrocatalytic Degradation of Sulfamethoxazole on G-C<sub>3</sub>N<sub>4</sub>/BiOI/EG P-N Heterojunction Photoanode under Visible Light Irradiation. *Appl. Surf. Sci.* 483 (January), 506–520. doi:10.1016/j.apsusc.2019.03.281
- Mao, L., Liu, H., Yao, L., Wen, W., Chen, M.-M., Zhang, X., et al. (2022). Construction of a Dual-Functional CuO/BiOCl Heterojunction for High-Efficiently Photoelectrochemical Biosensing and Photoelectrocatalytic Degradation of Aflatoxin B1. *Chem. Eng. J.* 429, 132297–138947. doi:10.1016/j.cej.2021.132297
- Martinez-Huitle, C. A., Rodrigo, M. A., Sirés, I., and Scialdone, O. (2015). Single and Coupled Electrochemical Processes and Reactors for the Abatement of Organic Water Pollutants: A Critical Review. *Chem. Rev.* 115 (24), 13362–13407. doi:10.1021/acs.chemrev.5b00361
- Monllor-Satoca, D., Díez-García, M. I., Lana-Villarreal, T., and Gómez, R. (2020). Photoelectrocatalytic Production of Solar Fuels with Semiconductor Oxides: Materials, Activity and Modeling. *Chem. Commun.* 56 (82), 12272–12289. doi:10.1039/d0cc04387g
- Mousset, E., and Dionysiou, D. D. (2020). Photoelectrochemical Reactors for Treatment of Water and Wastewater: a Review. *Environ. Chem. Lett.* 18 (4), 1301–1318. doi:10.1007/s10311-020-01014-9
- Nava-Núñez, M. Y., Jimenez-Relinque, E., Grande, M., Martínez-de la Cruz, A., and Castellote, M. (2020). Photocatalytic BiOX Mortars under Visible Light Irradiation: Compatibility, NO<sub>x</sub> Efficiency and Nitrate Selectivity. *Catal. Digit. Publ. Inst.* Vol. 1010 (2), 226226. doi:10.3390/CATAL10020226
- Nellist, M. R., Laskowski, F. A. L., Lin, F., Mills, T. J., and Boettcher, S. W. (2016). Semiconductor-Electrocatalyst Interfaces: Theory, Experiment, and Applications in Photoelectrochemical Water Splitting. *Acc. Chem. Res.* 49 (4), 733–740. doi:10.1021/acs.accounts.6b00001
- Nguyen, C. H., Tran, H. N., Fu, C.-C., Lu, Y.-T., and Juang, R.-S. (2020). Roles of Adsorption and Photocatalysis in Removing Organic Pollutants from Water by Activated Carbon-Supported Titania Composites: Kinetic Aspects. *J. Taiwan Inst. Chem. Eng.* 109, 51–61. doi:10.1016/j.jtice.2020.02.019
- Olea, M. A. U., Bueno, J. d. J. P., and Pérez, A. X. M. (2021). Nanometric and Surface Properties of Semiconductors Correlated to Photocatalysis and Photoelectrocatalysis Applied to Organic Pollutants - A Review. *J. Environ. Chem. Eng.* 9 (July), 106480. doi:10.1016/j.jece.2021.106480
- Orimolade, B. O., and Arotiba, O. A. (2022). Enhanced Photoelectrocatalytic Degradation of Diclofenac Sodium Using a System of Ag-BiVO<sub>4</sub>/BiOI Anode and Ag-BiOI Cathode. *Sci. Rep.* 12, 1–12. doi:10.1038/s41598-022-08213-0
- Orimolade, B. O., Koiki, B. A., Peleyeju, G. M., and Arotiba, O. A. (2019). Visible Light Driven Photoelectrocatalysis on a FTO/BiVO<sub>4</sub>/BiOI Anode for Water Treatment Involving Emerging Pharmaceutical Pollutants. *Electrochimica Acta* 307, 285–292. doi:10.1016/j.electacta.2019.03.217
- Pancielejko, A., Łuczak, J., Lisowski, W., Zaleska-Medynska, A., and Mazierski, P. (2021). Novel Two-step Synthesis Method of Thin Film Heterojunction of BiOBr/Bi<sub>2</sub>WO<sub>6</sub> with Improved Visible-Light-Driven Photocatalytic Activity. *Appl. Surf. Sci.* 569, 151082. doi:10.1016/j.apsusc.2021.151082
- Paquin, F., Rivnay, J., Salleo, A., Stingelin, N., and Silva-Acuña, C. (2015). Multi-phase Microstructures Drive Exciton Dissociation in Neat Semicrystalline Polymeric Semiconductors. *J. Mat. Chem. C* 3, 10715–10722. doi:10.1039/b000000x10.1039/c5tc02043c
- Peter, L. M., Walker, A. B., Bein, T., Hufnagel, A. G., and Kondofersky, I. (2020). Interpretation of Photocurrent Transients at Semiconductor Electrodes: Effects of Band-Edge Unpinning. *J. Electroanal. Chem.* 872, 114234. doi:10.1016/j.jelechem.2020.114234
- Poznyak, S. K., and Kulak, A. I. (1990). Photoelectrochemical Properties of Bismuth Oxyhalide Films. *Electrochimica Acta. Pergamon* 35 (11–12), 1941–1947. doi:10.1016/0013-4686(90)87103-9

- Qi, S., Liu, X., Ma, N., and Xu, H. (2021). Construction and Photocatalytic Properties of WS<sub>2</sub>/MOS<sub>2</sub>/BiOCl Heterojunction. *Chem. Phys. Lett.* 763, 138203. doi:10.1016/j.cplett.2020.138203
- Qin, H., Wang, K., Jiang, L., Li, J., Wu, X., and Zhang, G. (2020). Ultrasonic-assisted Fabrication of a Direct Z-Scheme BiOI/Bi<sub>2</sub>O<sub>4</sub> Heterojunction with Superior Visible Light-Responsive Photocatalytic Performance. *J. Alloys Compd.* 821, 153417. doi:10.1016/j.jallcom.2019.153417
- Quesada, H. B., Baptista, A. T. A., Cusioli, L. F., Seibert, D., de Oliveira Bezerra, C., and Bergamasco, R. (2019). Surface Water Pollution by Pharmaceuticals and an Alternative of Removal by Low-Cost Adsorbents: A Review. *Chemosphere* 222, 766–780. doi:10.1016/j.chemosphere.2019.02.009
- Rashid, J., Karim, S., Kumar, R., Barakat, M. A., Akram, B., Hussain, N., et al. (2020). A Facile Synthesis of Bismuth Oxychloride-Graphene Oxide Composite for Visible Light Photocatalysis of Aqueous Diclofenac Sodium. *Sci. Rep.* 10 (1), 11. doi:10.1038/s41598-020-71139-y
- Sanganyado, E., Lu, Z., and Fu, Q. (2017). Chiral pharmaceuticals: A review on their environmental occurrence and fate processes. *Water Research* 124, 527–542. doi:10.1016/j.watres.2017.08.003
- Shi, Y., Li, J., and Mao, C. (2021). Van Der Waals Gap-Rich BiOCl Atomic Layers Realizing Efficient, Pure-Water CO<sub>2</sub>-to-CO Photocatalysis. *Nat. Commun.* 12 (1), 1–10. doi:10.1038/s41467-021-26219-6
- Siahrostami, S., et al. (2017). One- or Two-Electron Water Oxidation, Hydroxyl Radical, or H<sub>2</sub>O<sub>2</sub> Evolution. *J. Phys. Chem. Lett.* 8 (6), 1157–1160. doi:10.1021/acs.jpcc.6b02924
- Sigcha-Pallo, C., Peralta-Hernandez, J. M., and Allulema-pullupaxi, p. (2022). Photoelectrocatalytic Degradation of Diclofenac with a Boron-Doped Diamond Electrode Modified with Titanium Dioxide as a Photoanode. *Environ. Res.* 212, 113362. doi:10.1016/j.envres.2022.113362
- Singh, N., and Goldsmith, B. R. (2020). Role of Electrocatalysis in the Remediation of Water Pollutants. *ACS Catal. Am. Chem. Soc.* 10 (5), 3365–3371. doi:10.1021/ACSCATAL.9B04167/ASSET/IMAGES/LARGE/CS9B04167\_0005
- Singh, S., Sharma, R., and Khanuja, M. (2018). A Review and Recent Developments on Strategies to Improve the Photocatalytic Elimination of Organic Dye Pollutants by BiOX (X=Cl, Br, I, F) Nanostructures. *Korean J. Chem. Eng.* 3535 (10), 101955–101968. doi:10.1007/S11814-018-0112-Y
- Stephenson, J., Cellorio, V., and Tiwari, D. (2018). Photoelectrochemical Properties of BiOCl Microplatelets. *J. Electroanal. Chem.* 819, 171–177. doi:10.1016/j.jelechem.2017.10.024
- Su, J., Xiao, Y., and Ren, M. (2014). Direct Hydrolysis Synthesis of BiOI Flowerlike Hierarchical Structures and Its Photocatalytic Activity under Simulated Sunlight Irradiation. *CATCOM* 45, 30–33. doi:10.1016/j.catcom.2013.10.020
- Sun, M., Hu, J., and Cai, C. (2017). CuI as Hole-Transport Channel for Enhancing Photoelectrocatalytic Activity by Constructing CuI/BiOI Heterojunction. *ACS Appl. Mater. Interfaces* 9 (15), 13223–13230. doi:10.1021/acsami.7b01840
- Tugaon, H. O., Grecia-Segurs, S., and Hristovaski, K. (2017). Challenges in Photocatalytic Reduction of Nitrate as a Water Treatment Technology. *Photocatal. Nanoparticle Nanotechnol. Sci. Total Environ.* 599, 1524–1551. doi:10.1016/j.scitotenv.2017.04.238
- Urban, J. J. (2017). Emerging Scientific and Engineering Opportunities within the Water-Energy Nexus. *Elsevier Inc.* 1 (4), 665–688. doi:10.1016/j.joule.2017.10.002
- Vargas, R., Carvajal, V., and Galavis, B. (2019). High-field Growth of Semiconducting Anodic Oxide Films on Metal Surfaces for Photocatalytic Application. *Int. J. Photoenergy.* doi:10.1155/2019/2571906
- Vasseghian, Y., Hosseinzadee, S., and Khattee, A. (2021). The Concentration of Persistent Organic Pollutants in Water Resources: A Global Systematic Review, Meta-Analysis and Probabilistic Risk Assessment. *Sci. Total Environ.* 796, 149000. doi:10.1016/j.scitotenv.2021.149000
- Wang, H., Liang, Y., and Liu, L. (2018). Highly Ordered TiO<sub>2</sub> Nanotube Arrays Wrapped with G-C<sub>3</sub>N<sub>4</sub> Nanoparticles for Efficient Charge Separation and Increased Photoelectrocatalytic Degradation of Phenol. *J. Hazard. Mater.* 344, 369–380. doi:10.1016/j.jhazmat.2017.10.044
- Wang, J., and Bai, Z. (2017). Fe-based catalysts for heterogeneous catalytic ozonation of emerging contaminants in water and wastewater. *Chemical Engineering Journal* 312, 79–98. doi:10.1016/j.cej.2016.11.118
- Wang, Q., Gao, Q., and Wu, H. (2019). *In Situ* construction of Semimetal Bi Modified BiOI-Bi<sub>2</sub>O<sub>3</sub> Film with Highly Enhanced Photoelectrocatalytic Performance. *Separation. Purification Tech.* 226 (June), 232–240. doi:10.1016/j.seppur.2019.06.002
- Wang, B. B., Song, Z., and Sun, L. (2021). A Review: Comparison of Multi-Air-Pollutant Removal by Advanced Oxidation Processes-Industrial Implementation for Catalytic Oxidation Processes. *Chem. Eng. J.* 409, 128136. doi:10.1016/j.cej.2020.128136
- Wang, H., H., Zhang, B., and Tang, Y. (2020). Recent Advances in Bismuth Oxyhalide-Based Functional Materials for Photoelectrochemical Sensing. *TrAC - Trends Anal. Chem.* 131, 116020. doi:10.1016/j.trac.2020.116020
- Wang, L. L., Wang, L., and Du, Y. (2021). Progress and Perspectives of Bismuth Oxyhalides in Catalytic Applications. *Mater. Today Phys.* 16. doi:10.1016/j.mtphys.2020.100294
- Wang, L. L., Min, X., and Zhu, X. (2020). Facile Construction of Novel BiOBr/Bi<sub>12</sub>O<sub>17</sub>Cl<sub>2</sub> Heterojunction Composites with Enhanced Photocatalytic Performance. *J. Colloid Interface Sci.* 560, 21–33. doi:10.1016/j.jcis.2019.10.048
- Wei, X., AKbar, M. U., and Rasa, A. (2021). A Review on Bismuth Oxyhalide Based Materials for Photocatalysis. *Nanoscale Adv.*, 3353–3372. doi:10.1039/d1na00223f
- Wilczewska, P., Malankowska, A., and Ryl, J. (2021). Morphology Regulation Mechanism and Enhancement of Photocatalytic Performance of BiOX (X = Cl, Br, I) via Mannitol-Assisted Synthesis. *Catalysts* 2021Vol. 1111 (3), 312312. doi:10.3390/CATAL11030312
- Wu, D., Wang, X., and Wang, H. (2019). Ultrasonic-assisted Synthesis of Two Dimensional BiOCl/MOS<sub>2</sub> with Tunable Band Gap and Fast Charge Separation for Enhanced Photocatalytic Performance under Visible Light. *J. Colloid Interface Sci.* 533, 539–547. doi:10.1016/j.jcis.2018.08.084
- Xiong, J., Song, P., and Di, J. (2020). Bismuth-rich Bismuth Oxyhalides: A New Opportunity to Trigger High-Efficiency Photocatalysis. *J. Mater. Chem. A* 8 (41), 21434–21454. doi:10.1039/d0ta06044e
- Xu, X., Zhou, M., and Du, X. (2019). Photoelectrochemical Degradation of 2,4-dichlorophenoxyacetic Acid Using Electrochemically Self-Doped Blue TiO<sub>2</sub> Nanotube Arrays with Formic Acid as Electrolyte. doi:10.1016/j.jhazmat.2019.12.1096
- Xu, H. Y., H. Y., Lu, D., and Tan, Q. (2020). Visible-light-driven Photocatalytic Degradation of Rhodamine B in Water by BiOCl<sub>x</sub>I<sub>1-x</sub> X Solid Solutions. *Water Sci. Technol.* 81 (5), 1080–1089. doi:10.2166/wst.2020.205
- Xu, Q., Q., Zhang, L., and Zheng, Q. (2020). S-scheme Heterojunction Photocatalyst. *Chem. Elsevier Inc.* 6 (7), 1543–1559. doi:10.1016/j.chempr.2020.06.010
- Yan, T., Liu, H., and Jin, Z. (2021). G-C<sub>3</sub>N<sub>4</sub>/α-Fe<sub>2</sub>O<sub>3</sub> Supported Zero-Dimensional CO<sub>3</sub>S<sub>4</sub> Nanoparticles Form S-Scheme Heterojunction Photocatalyst for Efficient Hydrogen Production. *Energy Fuels* 35 (1), 856–867. doi:10.1021/acs.energyfuels.0c03351
- Yang, Y., Zhang, C., and LAi, C. (2018). *Historical Perspective BiOX (X = Cl, Br, I) Photocatalytic Nanomaterials: Applications for Fuels and Environmental Management.* doi:10.1016/j.cis.2018.03.004
- Ye, K.-H., Chai, Z., and Gu, J. (2015). BiOI-BiVO<sub>4</sub> Photoanodes with Significantly Improved Solar Water Splitting Capability: P-N Junction to Expand Solar Adsorption Range and Facilitate Charge Carrier Dynamics. *Nano Energy* 18, 222–231. doi:10.1016/j.nanoen.2015.10.018
- Younis, S. A., Kwan, E. E., and Qasim, M. (2020). Metal-organic Framework as a Photocatalyst: Progress in Modulation Strategies and Environmental/energy Applications. *Prog. Energy Combust. Sci.* 81, 100870. doi:10.1016/j.peccs.2020.100870
- Yuan, Y., Gao, T., and Zhong, L. F. (2022). Fabrication of a Dual S-Scheme Bi<sub>7</sub>O<sub>9</sub>I<sub>3</sub>/g-C<sub>3</sub>N<sub>4</sub>/Bi<sub>3</sub>O<sub>4</sub>Cl Heterojunction with Enhanced Visible-Light-Driven Performance for Phenol Degradation. *Chemosphere* 287 (P2), 132241. doi:10.1016/j.chemosphere.2021.132241
- Zhang, J., Xie, T., and Zhong, L. F. (2021). Preferential and Efficient Degradation of Phenolic Pollutants with Cooperative Hydrogen-Bond Interactions in Photocatalytic Process. *Chemosphere* 269, 129404. doi:10.1016/j.chemosphere.2020.129404
- Zhang, M., Yin, H. F., and Yao, J. F. (2020). All-solid-state Z-Scheme BiOX(Cl, Br)-Au-CdS Heterostructure: Photocatalytic Activity and Degradation Pathway. *Colloids Surfaces A Physicochem. Eng. Aspects* 602 (June), 124778. doi:10.1016/j.colsurfa.2020.124778

- Zhang, Xi, Ai, Z., and Zia, F. (2008). Generalized One-Pot Synthesis, Characterization, and Photocatalytic Activity of Hierarchical BiOX (X = Cl, Br, I) Nanoplate Microspheres. *J. Phys. Chem.* 112 (3), 747–753. doi:10.1021/JP077471T
- Zhao, C., Liu, y., and Chu, H. (2021). Construction of Direct Z-Scheme Bi<sub>5</sub>O<sub>7</sub>I/UiO-66-NH<sub>2</sub> Heterojunction Photocatalysts for Enhanced Degradation of Ciprofloxacin: Mechanism Insight, Pathway Analysis and Toxicity Evaluation. *J. Hazard. Mater.* 419 (June), 126466. doi:10.1016/j.jhazmat.2021.126466
- Zhao, L., Xang, Z., and Fan, C. (2012). First-principles Study on the Structural, Electronic and Optical Properties of BiOX (X=Cl, Br, I) Crystals. *Phys. B Condens. Matter* 407 (17), 3364–3370. doi:10.1016/j.physb.2012.04.039
- Zhu, Y., Xu, J., and Chen, M. (2022). Synthesis of La<sub>2</sub> Ti<sub>2</sub> O<sub>7</sub>/Bi<sub>5</sub> O<sub>7</sub> I Photocatalysts with Improved Photocatalytic Activity for Degradation of CIP under Visible Light. *Sep. Purif. Technol.* 282, 1383–5866. doi:10.1016/j.seppur.2021.120004

**Conflict of Interest:** The authors declare that the research was conducted in the absence of any commercial or financial relationships that could be construed as a potential conflict of interest.

**Publisher's Note:** All claims expressed in this article are solely those of the authors and do not necessarily represent those of their affiliated organizations, or those of the publisher, the editors and the reviewers. Any product that may be evaluated in this article, or claim that may be made by its manufacturer, is not guaranteed or endorsed by the publisher.

Copyright © 2022 Castillo-Cabrera, Espinoza-Montero, Alulema-Pullupaxi, Mora and Villacís-García. This is an open-access article distributed under the terms of the Creative Commons Attribution License (CC BY). The use, distribution or reproduction in other forums is permitted, provided the original author(s) and the copyright owner(s) are credited and that the original publication in this journal is cited, in accordance with accepted academic practice. No use, distribution or reproduction is permitted which does not comply with these terms.